Application de la spectroscopie à l'étude des décharges électriques dans les milieux denses.

N Bonifaci

CNRS, G2Elab, F-38000Grenoble, France
Nelly.Bonifaci@g2elab.grenoble-inp.fr

Joel Rosato, Jussi Eloranta, Zhiling Li , Vladimir Atrazhev, Vyacheslav Shakatov, Sebastien Flury

G2E. Lab covers the wide spectrum of the electrical engineering science

Application : Discharge in liquid

The plasma produced by electrical discharges in liquids are finding important applications in modern technology :
Electrical Insulation, High power switching, Electro discharge machning
Nanomaterials synthesis, Water sterilization, Plasma medecine

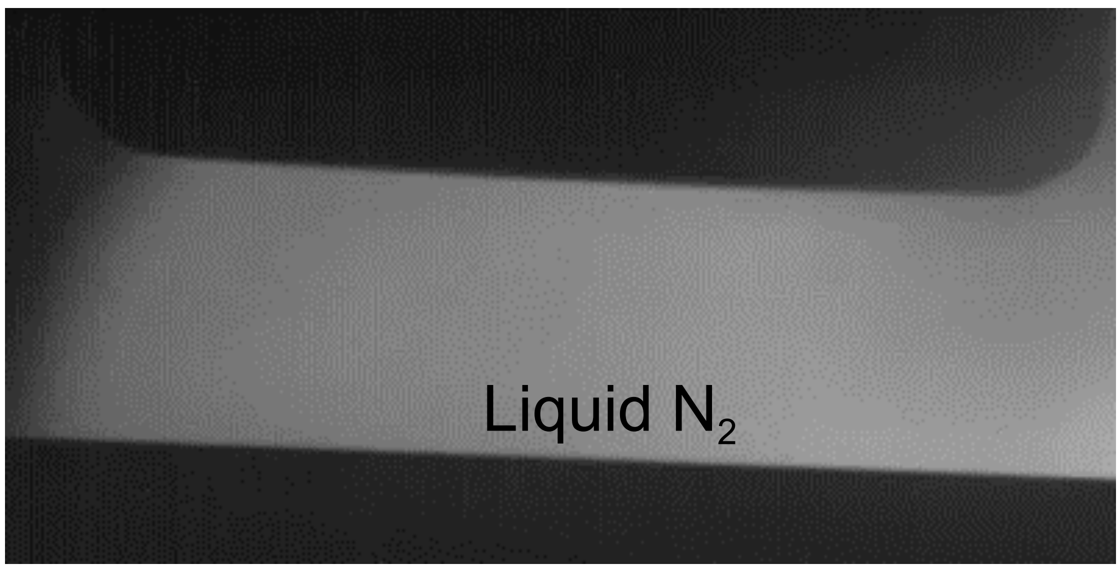

OES

- Continuum

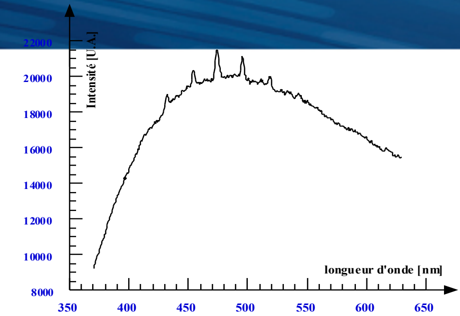

- Molecular spectra

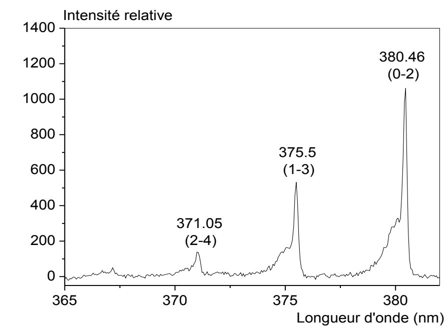

B. Pearse and A. G. Gaydon
The identification of Molecular Spectra Chapman and Hall 1976

G. Herzberg, *Molecular Spectra and Molecular Structure: I. Spectra of Diatomic Molecules*, 2nd edn. (Van Nostrand, Princeton, NJ, 1950)

I. Kovacs, *Rotational structure in the spectra of diatomic molecules* (Adam Higer Ltd., London, 1969)

- Atomic spectra

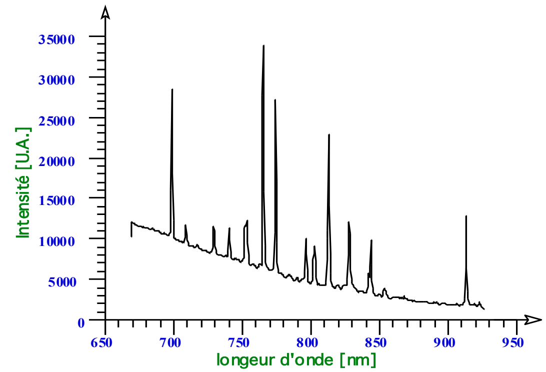

R. Stringanow and N. S. Sventitskii, Tables of Spectral Lines of Neutral and Ionized Atoms Plenum New York 1968.

NIST ASD Output: Lines http://physics.nist.gov/cgi-bin/ASD/lines1.pl

Atomic Spectral Line Database http://cfa-www.havard.edu/

Spectral Line Profile

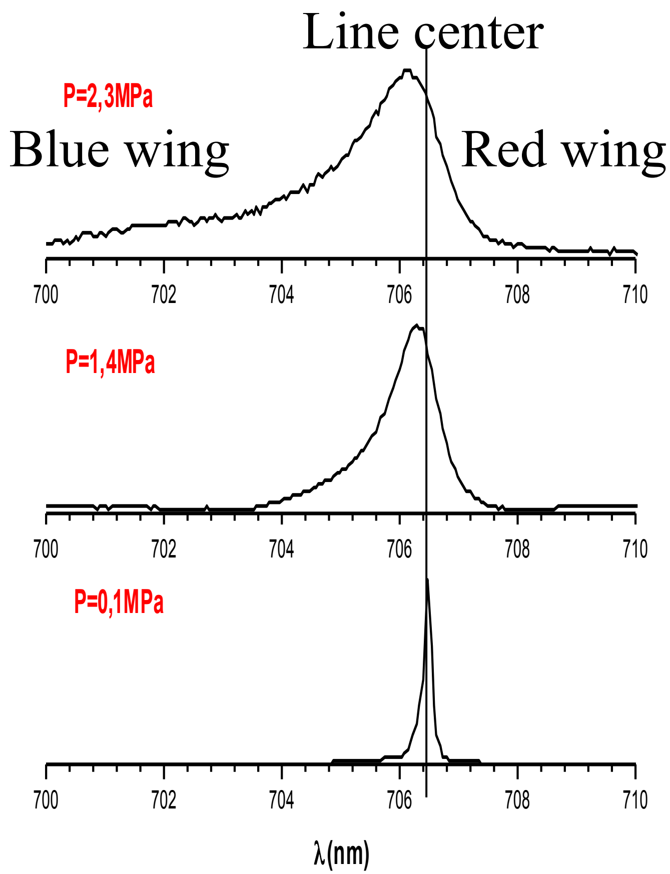

Line width $\Delta\lambda_{FWHM}$

Line shift $d=\lambda_{max}-\lambda_{vacuum}$

Asymmetry

Satellite band

Forbidden line

Self-absorption

Microscopic probe

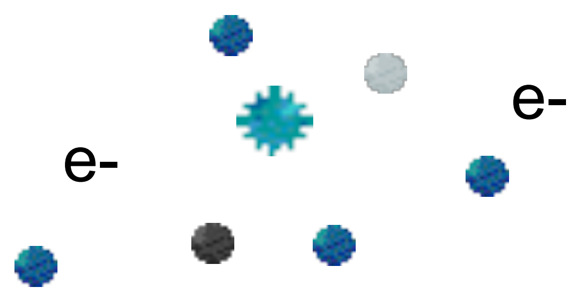

Broadening mechanisms

Natural Broadening

$$\cancel{\Delta\lambda_{natural} \sim 10^{-4}} \text{ Å}$$

Doppler Broadening

$$\Delta\lambda_D = 2\lambda\sqrt{\frac{2kTLn2}{Mc^2}} = 7.157\times10^{-7}\lambda\sqrt{\frac{T}{M}}$$

Gaussian Profile

Particle Temperature

	T	$\Delta\lambda_D$
He	10000	0,02 nm
Ar	10000	0,0057 nm
H_β	5000	0,025 nm

Instrumental Broadening

Gaussian profile

Pressure Broadening

Pressure Broadening

> The radiation emitted from an atom is changed by the force field of a neighboring atom. Frequency and amplitude are therefore no longer constant in time.... The change is so great, however, that the phase of the vibration after the collision is no longer the same as it would have been had there been no collision.
>
> —Weisskopf, 1933

Stark
Neutral (van der Waals)
Resonant

Semi empirical potential

$$V\left(r\right) = \pm \frac{\mathrm{h}C_p^{\omega}}{r^p} = \pm \frac{hC_p^{\nu}}{r^p}$$

$$m^p s^{-1}$$

ab initio potential

Semi empirical Potential

Linear Stark	$V(r) = \pm \frac{\hbar C_2^{\omega}}{r^2}$	-------
Quadratic Stark	$V(r) = \pm \frac{\hbar C_4^{\omega}}{r^4}$	-------
Resonant	$V(r) = \pm \frac{\hbar C_3^{\omega}}{r^3}$	$C_3^{\omega} = \frac{e^2 f_r \lambda_r}{16\pi^2 \varepsilon_0 m_e c}$
van der Waals	$V(r) = -\frac{\hbar C_6^{\omega}}{r^6}$	$C_6^{\omega} = \frac{1}{2h\varepsilon_0} e^2 \alpha \left\| \langle r^2 \rangle \right\|$ $m^6 s^{-1}$ $C_6^{\omega} = e^2 \alpha \left\| \langle r^2 \rangle \right\|$ ergcm^6 α atomic polarizability m^3 $\langle r^2 \rangle = a_0^2 \frac{n^{*2}}{2z_i^2} \langle 5n^{*2} + 1 - l(l+1) \rangle$ $n^* = \sqrt{z_i \frac{E_H}{E_i - E_u}}$
~~L-J~~	$V(r) = \hbar \left(\frac{C_{12}}{r^{12}} - \frac{C_6^{\omega}}{r^6} \right)$	W. Behmenburg J. Quant. Spectrosc. Radiat. Transfer 4, (1964) 177 W. R. Hindmarsh, A. D. Petford, G. Smith, Proc Roy Soc A 297 (1967) 296 W. R. Hindmarsh, A. N. Du Plessis et J. M. Farr (1970) J. Phys. B: At. Mol. Opt. Phys. 3, L5-L8 Butaux, F Schuller, R Lennuier J de Phys, 33, (1972), 635.

H G Kuhn : Does your treatment predict satellite line?
A Jablonski: The theory does not predict this mysterious effect.   1968

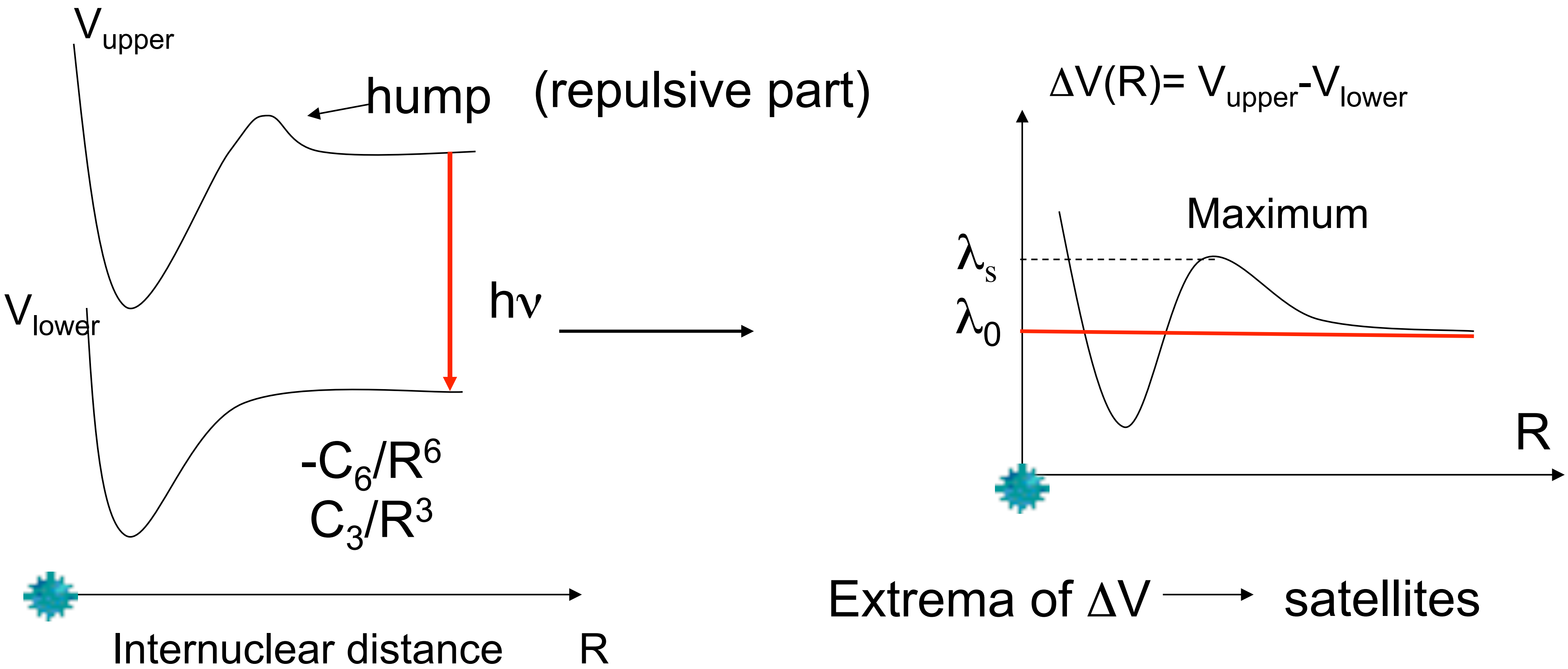

Extrema of $\Delta V \longrightarrow$ satellites

Maximum of $\Delta V \longrightarrow$ Blue satellites

MOLPRO 2009 package
http://www.molpro.net
Laboratoire de Physique et Chimie Quantique Toulouse

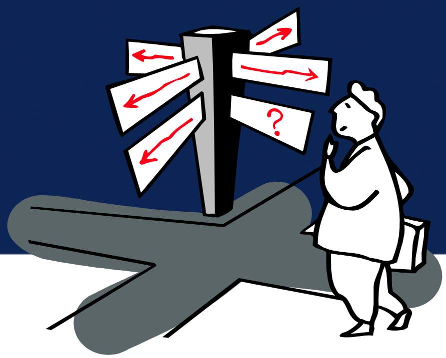

Interaction
Physical classification

Stark
Van der Waals ($-C_6/r^6$)
Resonant ($+-C_3/r^3$)

Potentiel ab initio

Spectral line Profile

?

Historical development

Impact approximation Phase shift

Weisskopf (1932), Lindholm (1941), Foley (1946)

$$\omega(t) = \omega_0 + \frac{d\eta}{dt}$$

Quasistatic approximation

Holtsmark (1919), Kuhn and Margenau (1937),

$$\omega = \omega_0 + \frac{\Delta V(r)}{h}$$

Line shape formalism based on the Fourier transform of the autocorrelation function

$$P(\omega) = \frac{1}{\pi}\mathrm{Re}\int_0^{+\infty}\phi(\tau)\exp[i\omega\tau]d\tau$$

$$\phi(\tau) = \int_{-\infty}^{+\infty} e^{i(\eta(t)-\eta(t-\tau))}dt$$

P. W. Anderson, Phys Rev 76 (1949) 647.
P. W. Anderson, Phys Rev 86 (1952) 809.

Autocorrelation function (wave train)

Spectral Line Profile

Quantum treatment

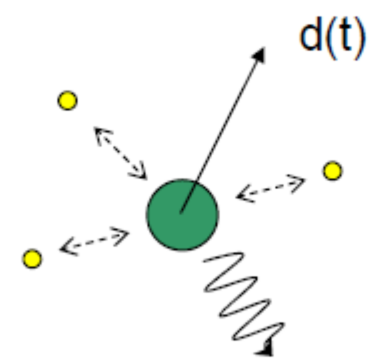

$$I(\omega) = \frac{1}{\pi}\mathrm{Re}\int_0^{\infty} dt \left\langle \vec{d}(0)\cdot\vec{d}(t)\right\rangle e^{i\omega t}$$

d is the dipole moment

U(t) evolution operator relative to the electrons

$$\vec{d}(t) = U^{+}(t)\vec{d}(0)U(t)$$

U-matrix

$$i\hbar\frac{dU}{dt}(t) = (H_0(t) + V(t))U(t)$$

H_0 is the Hamiltonian of the unperturbed emitter

time-dependent Schrödinger equation for the evolution operator U(t) $\longrightarrow$ **Code**

Spectral Line Profile

Classical theory

$$P(\omega) = \frac{1}{\pi} \mathrm{Re} \int_0^{+\infty} \phi(\tau) \exp[i\omega\tau] d\tau$$

$$\phi(\tau) = \int_{-\infty}^{+\infty} e^{i(\eta(t)-\eta(t-\tau))} dt$$

$$\phi(\tau) = \left\langle e^{-i\eta} \right\rangle_t = e^{-N_{pert} V_p(\tau)}$$

Isolated line!!

This concerns most of atomic lines emitted from non-hydrogenic systems.

$$\left\langle \vec{d}(0) \cdot \vec{d}(t) \right\rangle \propto \left\{ e^{-i\eta(t)} \right\} e^{-i\omega_{ul} t}$$

Autocorrelation function (wave train)

The autocorrelation function measures the average evolution of the wave train over a time interval τ from an initial time t

Spectral Line Profile

$$\phi(\tau) = \left\langle e^{-i\eta} \right\rangle_t = e^{-N_{pert} V_p(\tau)}$$

Perturber density N_{pert}

V_p: collision volume

$$V_p(\tau) = 2\pi\left[\int_0^{+\infty} b\,db \int_{-\infty}^{+\infty} dx \,\left\{ 1 - \exp\left(-i\frac{1}{\hbar}\int_0^{\tau} V\,(R(t'))dt'\right) \right\}\right]$$

$$R(t) = \left[b^2 + \left(x_0 + \bar{v}t\right)^2\right]^{1/2}$$

b is the impact parameter

Rectilinear classical path

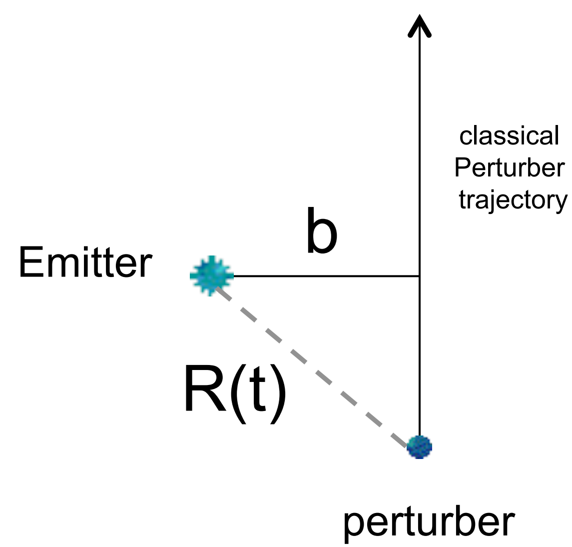

Unified theory

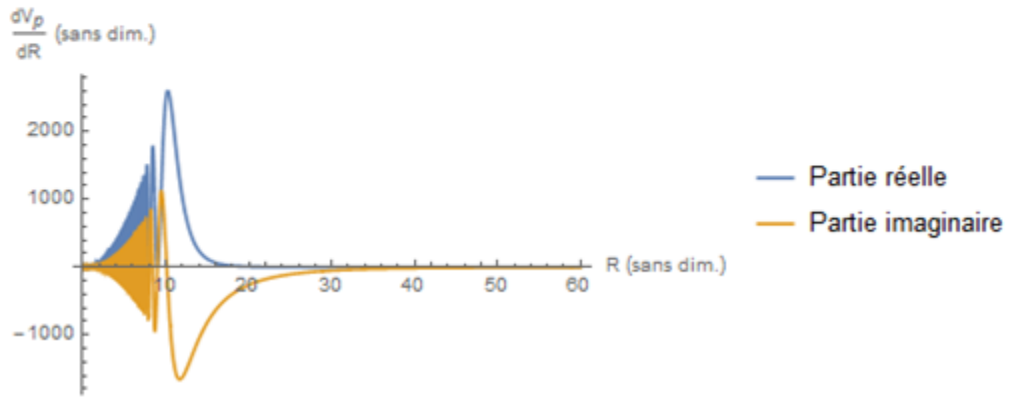

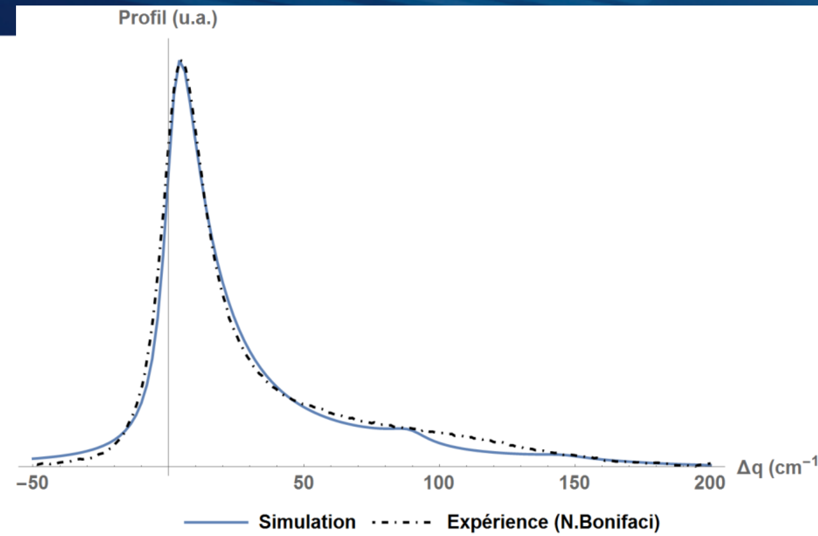

$$g_{(i,f)}(\tau) = \frac{1}{\sum_{ee'}^{\alpha} \left| d_{ee'} \right|^2} \sum_{ee'}^{\alpha} \int_0^{\infty} 2\pi\rho\, d\rho \int_{-\infty}^{+\infty} dx\, d_{ee'}(R(0)) \left[e^{\frac{i}{\hbar}\int_0^{\tau} dt \mathbf{V}(R(t))} \tilde{d}^{*}_{e'e}(R(\tau)) - \tilde{d}_{ee'}(R(0)) \right]$$

$$\tilde{d}_{ee'}\left(R(t)\right) = d_{ee'}\left[R(t)\right] e^{-\frac{1}{kT} V_e \left[R(t)\right]}$$

$d_{ee'}$ Dipole transition moment (ab initio calculation)

Allard N F, Royer A, Kielkopf J F and Feautrier N 1999 Phys. Rev. A 60 1021

Spectral Line Profile

Experimental profile		
Lorenztian profile (Voigt profile)	Impact approximation	N<<, core
Red Asymmetric profile	Quasi static approximation	N>>, wing
	Unified theory	N, ω

The quasistatic and impact approximations represent important theoretical limits that are in many cases sufficient for practical purposes and have been used to guide and develop new methods that are more generally applicable and, in fact, satisfactorily solve the line broadening problem in practically all cases.

S. Alexiou / (2009)

Impact Approximation

Stark	--------
Resonant	$$\Delta\lambda_{res} = K\frac{1}{\pi}\sqrt{\frac{g_0}{g_r}}\frac{e^2\lambda_{ul}^2 f_r\lambda_r}{4\pi\varepsilon_0 m_e c^2}N \propto \frac{P}{T}$$ $$S_{\lambda res} \approx 0$$ K: 0,9-1,8
van der Waals	$$\Delta\lambda_{vdw} = A\left(\frac{\lambda_{ul}^2}{2\pi c}\right)\Delta C_6^{2/5}\bar{v}^{3/5}N \propto \frac{P}{T^{0.7}}$$ A : 8.08 ou 8.16 $$S_{\lambda vdw} = \frac{\Delta\lambda_{VDW}}{2,75}$$ $$\bar{v} = \sqrt{8kT/\pi\mu}$$

Quasistatic Approximation

<table>
<tr><td>Stark</td><td>--------</td></tr>
<tr><td>Resonant</td><td>

$$\Delta\lambda_{resQS} = \Delta\lambda_{res}\left(1-\beta N\right) \qquad S_{\lambda res QS} \approx \varepsilon \Delta\lambda_{resQS}$$

H. R. Zaidi , Can. J. Physics 55, (1977) 1243.

</td></tr>
<tr><td>Van der Waals</td><td>

$$\Delta\lambda_{QS} = 0.411\pi^2 C_6 \frac{\lambda_{ul}^2}{c} N^2$$

$$\begin{cases} P_{QS}(\lambda) = \dfrac{1}{2}\left(\dfrac{\Delta\lambda_{qs}}{(\lambda-\lambda_{ul})^3}\right)^{1/2} \exp\left(-\dfrac{\pi}{4}\dfrac{\Delta\lambda_{qs}}{(\lambda-\lambda_{ul})}\right) & \lambda > \lambda_{ul} \\ P_{QS}(\lambda) = 0 & \lambda \le \lambda_{ul} \end{cases}$$

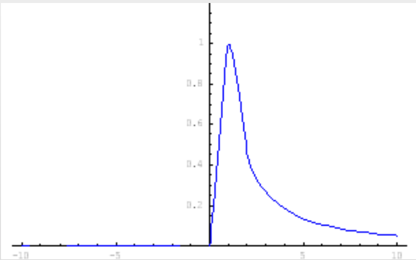

$$P_T = \int_{-\infty}^{+\infty} P_{Lor}(\Delta\lambda - \zeta) P_{QS}(\zeta) d\zeta$$

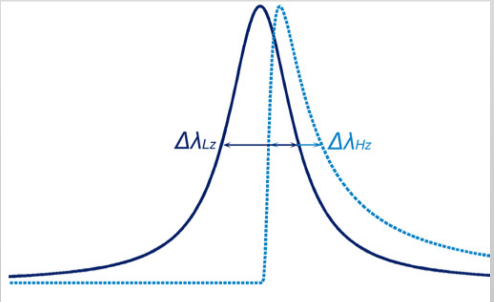

H. Margenau Phys. Rev. 48, (1935) 755.
H. Margenau Phys Rev 82 (1951) 156.

</td></tr>
</table>

Stark

Linear Stark effect   Hydrogen lines

H_α 656.2 nm, H_β 486.1 nm

H.R. Griem, Plasma Spectroscopy, Academic Press, New York, 1964.1964 H Griem Spectral line broadening by Plasmas London Academic 1974 H. Griem, Principles of Plasma Spectroscopy, Cambridge University Press, 1997.	$N_e = C(N_e, T) * \Delta\lambda^{3/2}$ Where $C(N_e,T)$ is in $A^{-3/2}$ cm^{-3}.
M. Gigosos et V. Gardeñoso, J. Phys. B: At. Mol. Opt. Phys., vol. 29, no 20, p. 4795, oct. 1996. M. Gigosos , M Gonzalez V. Gardeñoso Spectrochimica Acta Part B 58 (2003) 1489–1504	H_α $\left\{ \begin{array}{l} \text{Table} \\ \text{full width at half area} \end{array} \right.$ H_β $\Delta\lambda_{stark}(nm) = 4.8\left(\frac{N_e}{10^{23}}\right)^{0.68116}$

Example : Helium Gas
Linear Stark effect + van der Waals

$$\Delta\lambda_{lor} = \Delta\lambda_{stark}\left(N_e, T_e\right) + \Delta\lambda_{vdw}\left(N\right)$$

H-β	C_6 [m^6s^{-1}]	$\Delta\lambda_{vdw}$
4s-2p	$7.59*10^{-43}$	$2.20\times10^{-5}PT^{-7/10}$
4p-2s	$6.85*10^{-43}$	$2.12\times10^{-5}PT^{-7/10}$
4d-2p	$5.82*10^{-43}$	$1.98\times10^{-5}PT^{-7/10}$

H-α	C_6 [m^6s^{-1}]	$\Delta\lambda_{vdw}$
3s-2p	$2.75*10^{-43}$	$2.40\times10^{-5}PT^{-7/10}$
3p-2s	$1.696*10^{-43}$	$2.20\times10^{-5}PT^{-7/10}$
3d-2p	$1.18*10^{-43}$	$1.93\times10^{-5}PT^{-7/10}$

H_β quadratic Stark, H_α self –absorption

Quadratic Stark Effect

Impact Approximation

electrons

Quasistatic Approximation

ions

$$J(x) = \frac{1}{\pi}\int_0^\infty \frac{\mathrm{W}(\beta)d\beta}{1+\left(x - A^{4/3}\beta^2\right)^2}$$

Holtsmark distribution

$$W(\beta) = (2/\pi)\beta\int_0^\infty \chi \sin(\beta\chi)\exp\left(-\chi^{3/2}\right)d\chi$$

$$\Delta\lambda_{Stark} = (1+1.75\alpha(1-0.75r))2\omega$$

$$S_{\lambda(Stark)} = d \pm 2A(1-0{,}75r)\omega$$

$\Longrightarrow$ $\mathbf{N_e}$, $\mathbf{T_e}$ p. 97 Griem 1974

- H. R. Griem (1964) Plasmas Spectroscopy , McGraw-Hill Book Compagny, New York.
- H .R. Griem (1974) Spectral Line Broadening by Plasmas , New York : Academic Press.
- H. R. Griem (1997) Principles of Plasma Spectroscopy , Cambridge.

Stark : Line shape Code

Quantum treatment, Numerical calculation

Simulation code	**LSNS**	Rosato, J. et al J. Quant. Spectrosc. Radiat. Transfer **2015**, 165, 102–107	**computer simulation method** The particle motion is simulated and the Schrödinger Eq. is solved numerically it is time consuming	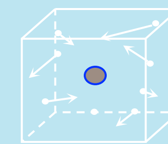
	SimU	Stambulchik, E. et al Phys. Rev. E **2007**, 75, 016401		
	.....			
Models	**PPP**	Calisti, A et al Phys. Rev. A **1990**, 42, 5433–5440.	Frequency Fluctuation Model Rapid calculations for neutral and charged emitters	
	QC-FFM	Stambulchik, E.et al Phys. Rev. E **2013**, 87, 053108.	Frequency Fluctuation Model	
	Zest	Gilleron, F et al Atoms **2018**, 6, 11	Quasi-static description of ions and impact approximation for electrons	
	......			

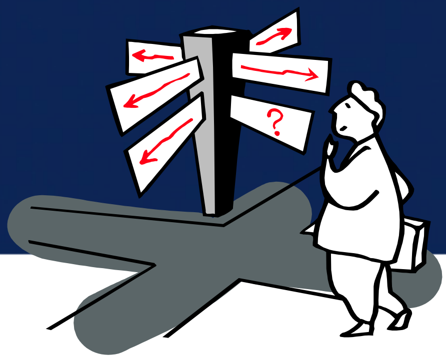

Interaction
Physical classification

Stark (C_2/r^2, C_4/r^4)
Van der Waals ($-C_6/r^6$)
Resonant ($\pm C_3/r^3$)

Potentiel ab initio
Code MOLPRO
http://www.molpro.net

Spectral line Profile

Quantum treatment

Classical theory

- Unified theory
- Impact approximation
- Quasitatic approximation

Examples

1. **Self-healing of a metallized polypropylene film**
2. **Positive streamers in liquid nitrogen**
3. **Streamers in chlorinated alkane and alkene liquids**
4. **Helium cryoplasma**

Modeling of the spectroscopic emission lines of Aluminum emitted by a self-healing of a metallized polypropylene film.

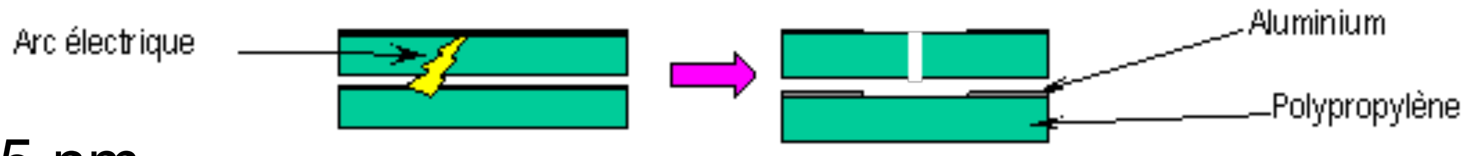

394.5 and 396.15 nm

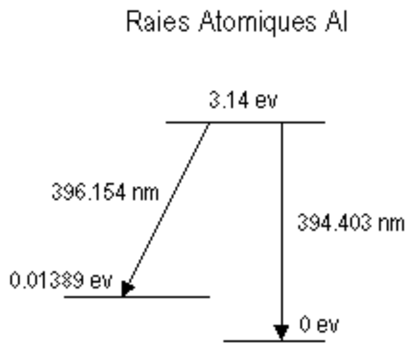

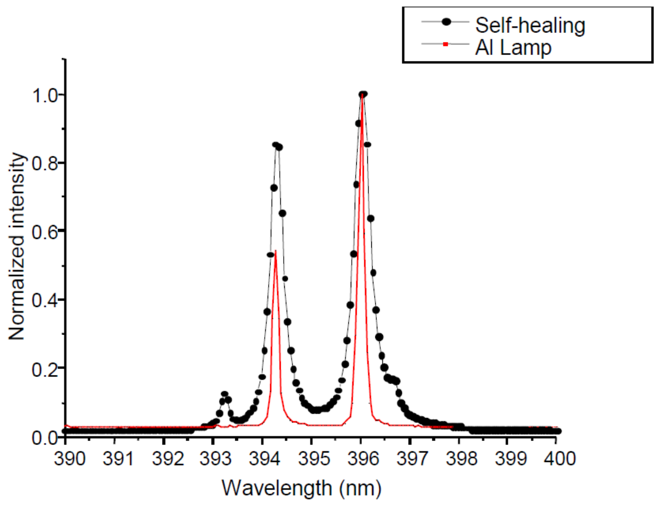

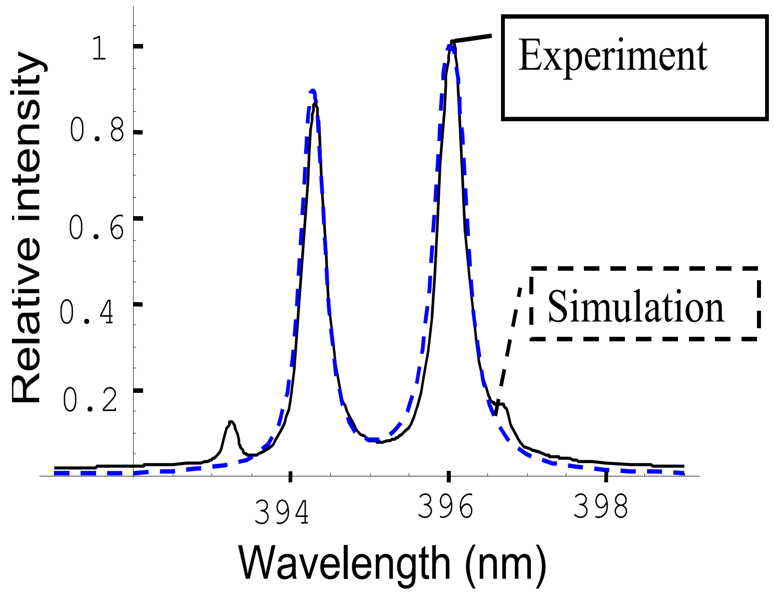

Modeling of the spectroscopic emission lines of Aluminum emitted by a self-healing of a metallized polypropylene film.

Confined discharge

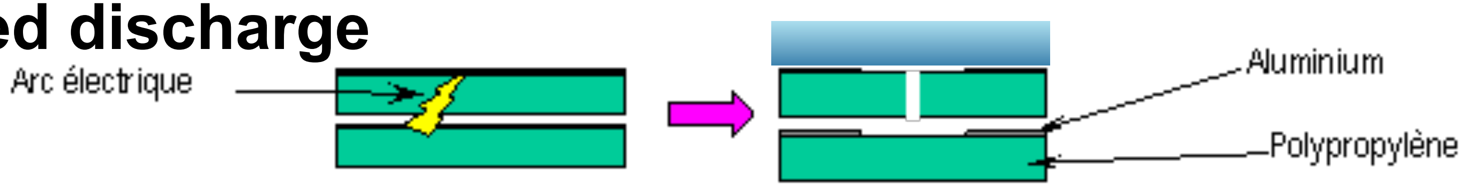

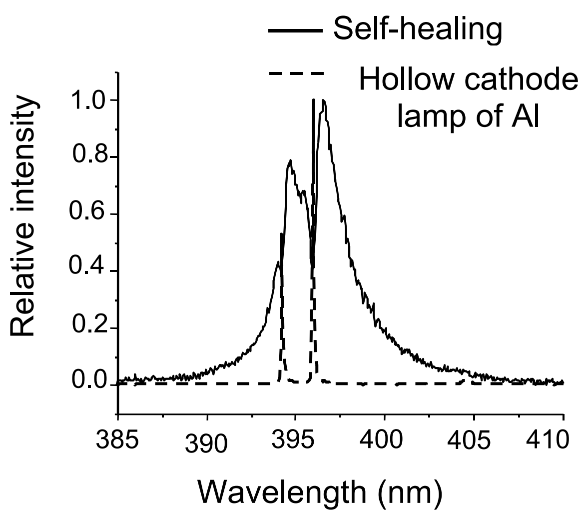

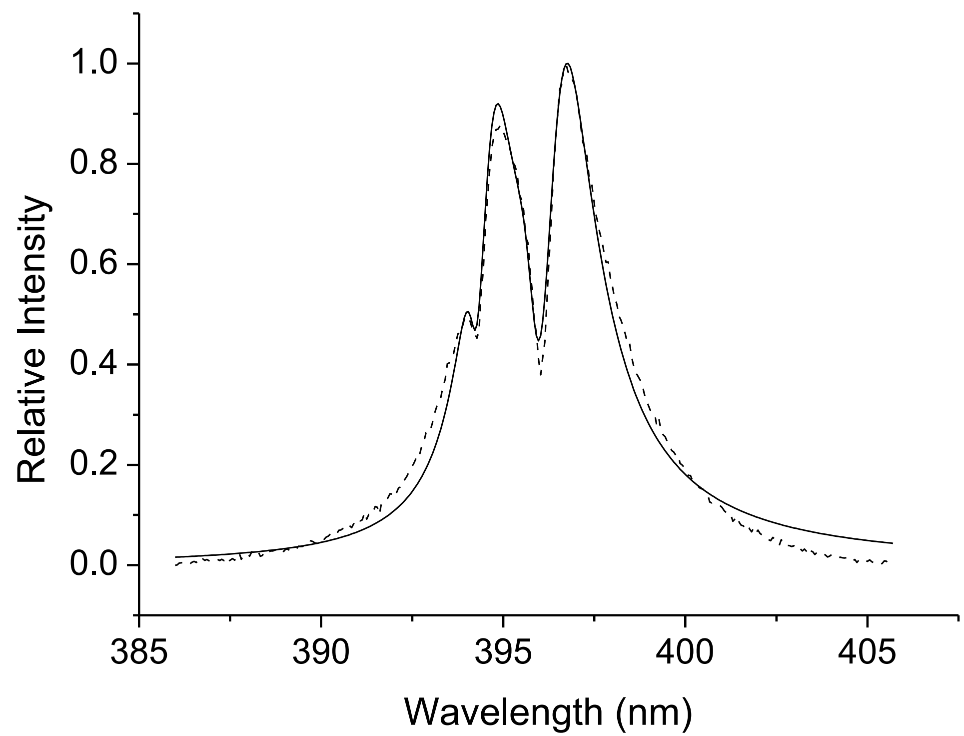

T=6500-7000K

N_g=0,8-1 10^{26} m^{-3}

N_e=2-3 10^{24} m^{-3}

Positive filamentary streamers in liquid nitrogen

Two distinct phases

0,4/1400µs
100-200 mA

80mm, 102kV

d

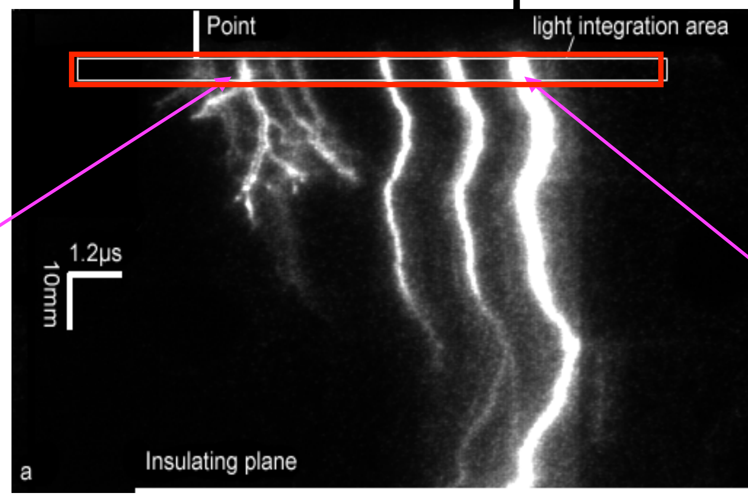

Streak photograph of filamentary streamer propagating up to plane

The streamer propagation

Weak emitted light

~100 streamers

Streamer reaches the plane
Re-illumination

Intense emitted light

1 streamer

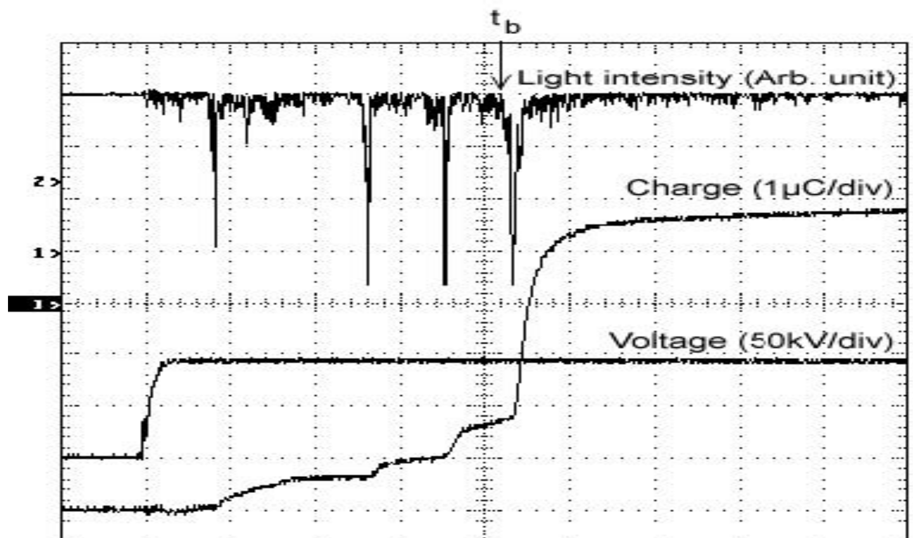

Positive filamentary streamers in liquid nitrogen

Experimental Results

Re-illumination

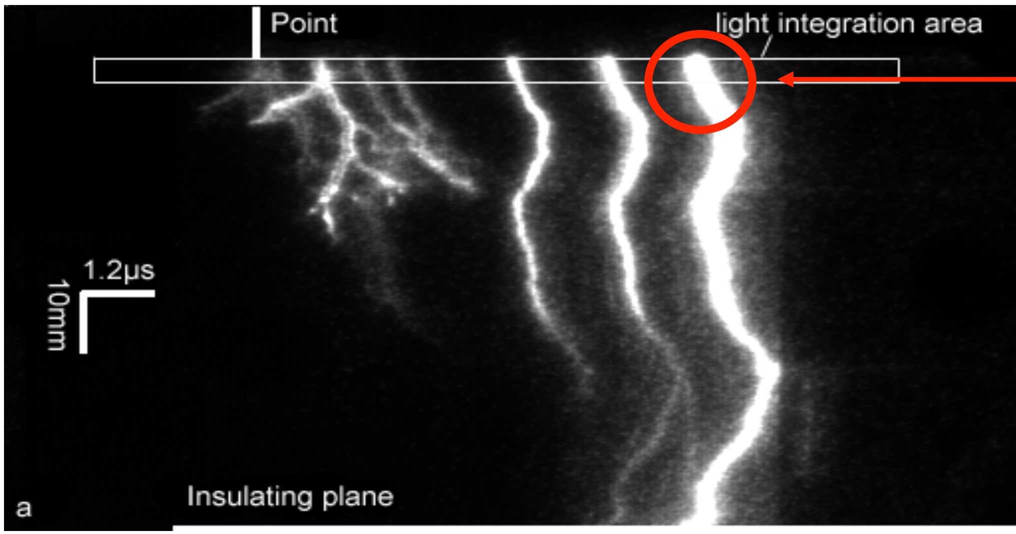

time

T=0

$T_{breakdown}$

Light emitted by one positive streamer in LN_2 when it stops on the insulating plane

Intense NI Atomic line

($3s^4P$-$3p^4S^0$ and $3s^4P$-$3p^4P$ transition)

No N_2 emission

When one positive streamer stops on the insulating plane,
a large current pulse and a bright emitted light are recorded at t_b

Positive filamentary streamers in liquid nitrogen

Re-illumination

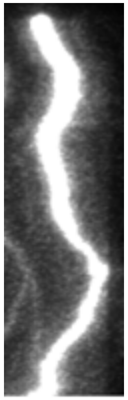

Propagation velocity : 10-30 km/s

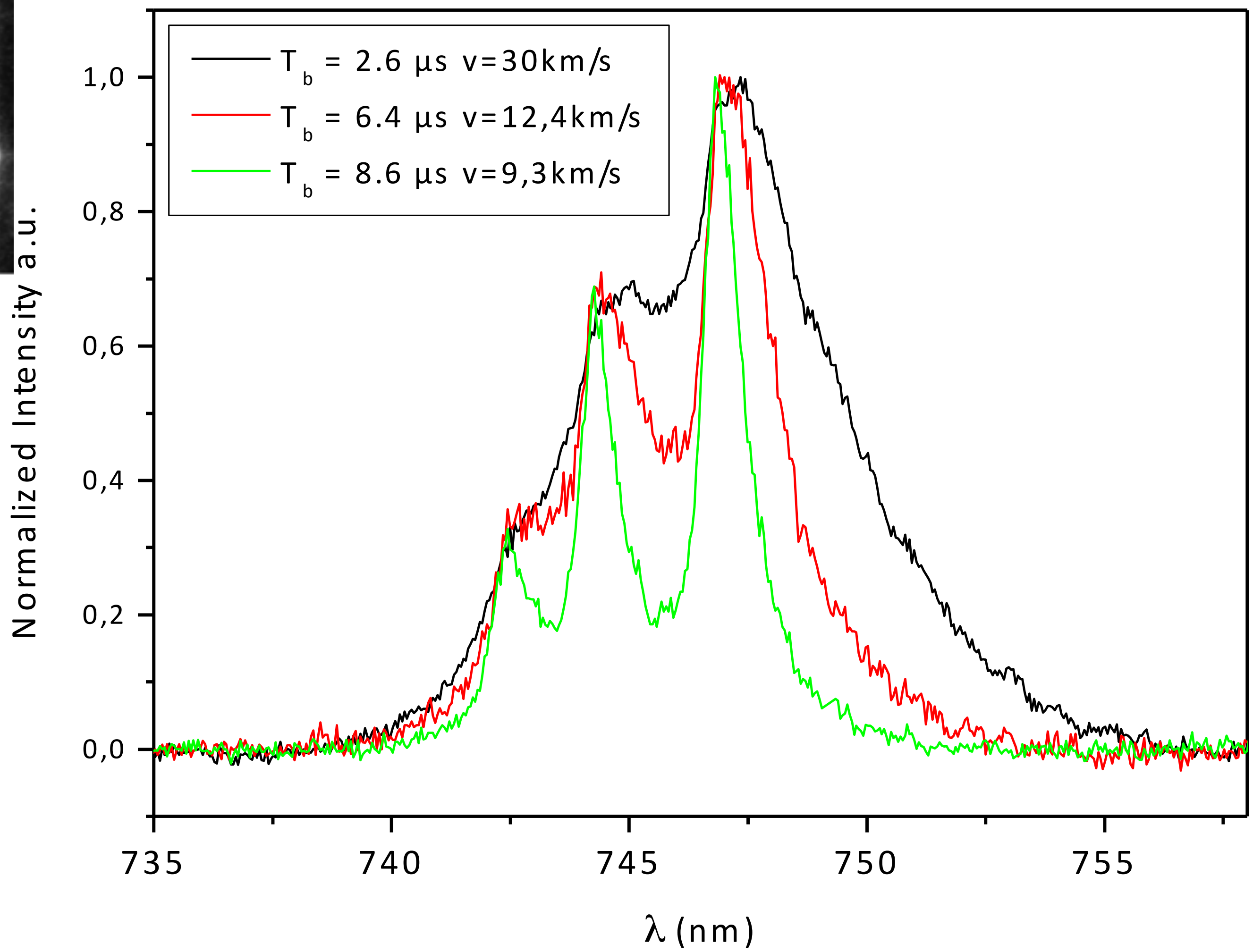

Broadening of Atomic line of NI

Positive filamentary streamers in liquid nitrogen

Re-illumination

Simulation of atomic line

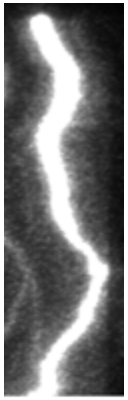

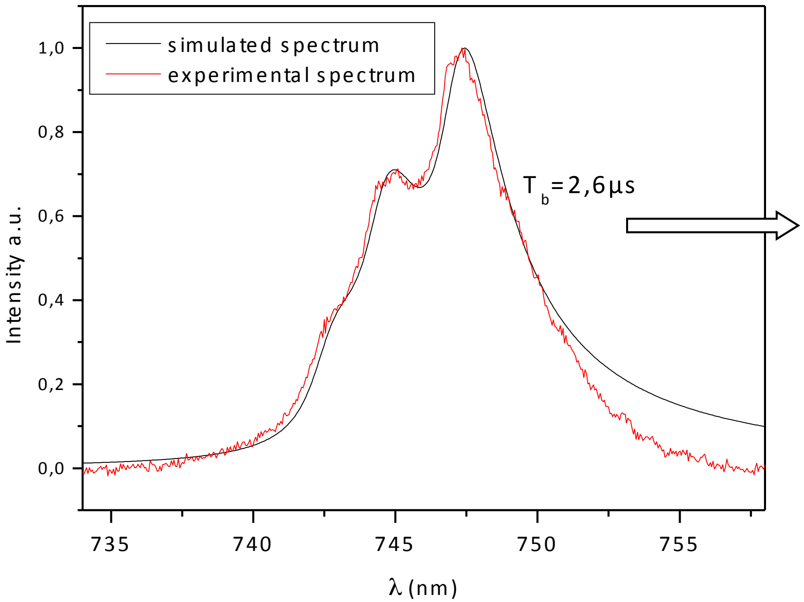

$N_e \sim 1,5x10^{24}\ m^{-3}$

$N_g \sim 6x10^{26}\ m^{-3}$

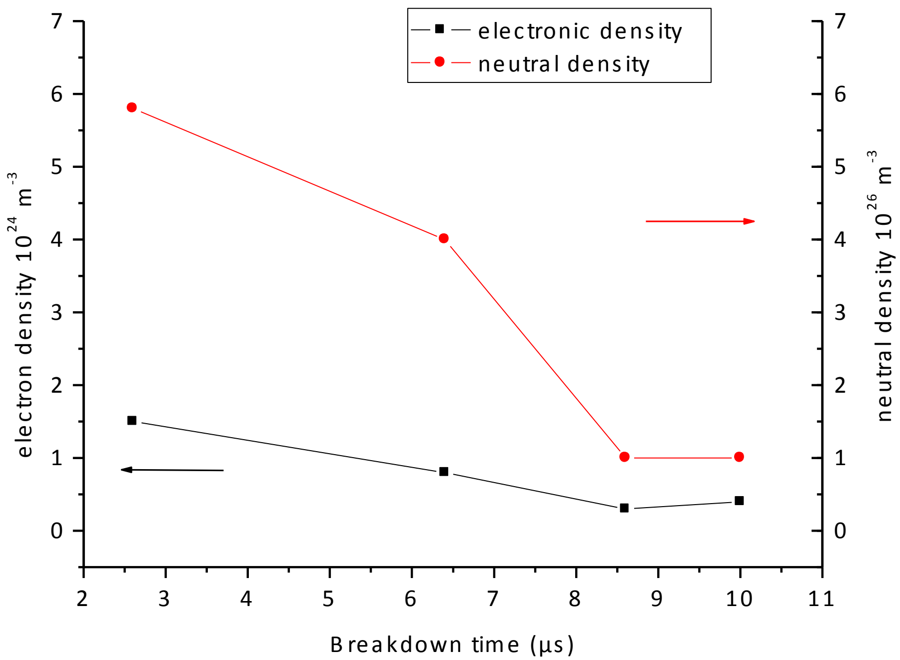

Positive filamentary streamers in liquid nitrogen

Re-illumination

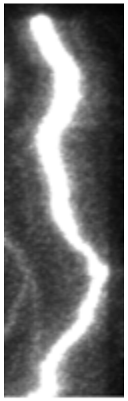

N_g (2.6µs) > N_g (8.6µs) ?

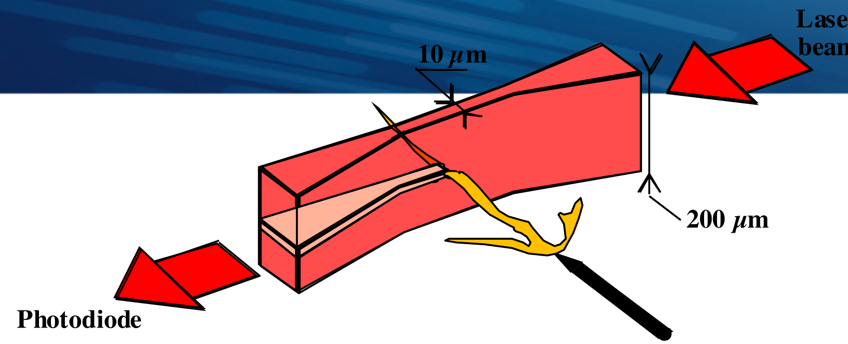

streamer channel radius

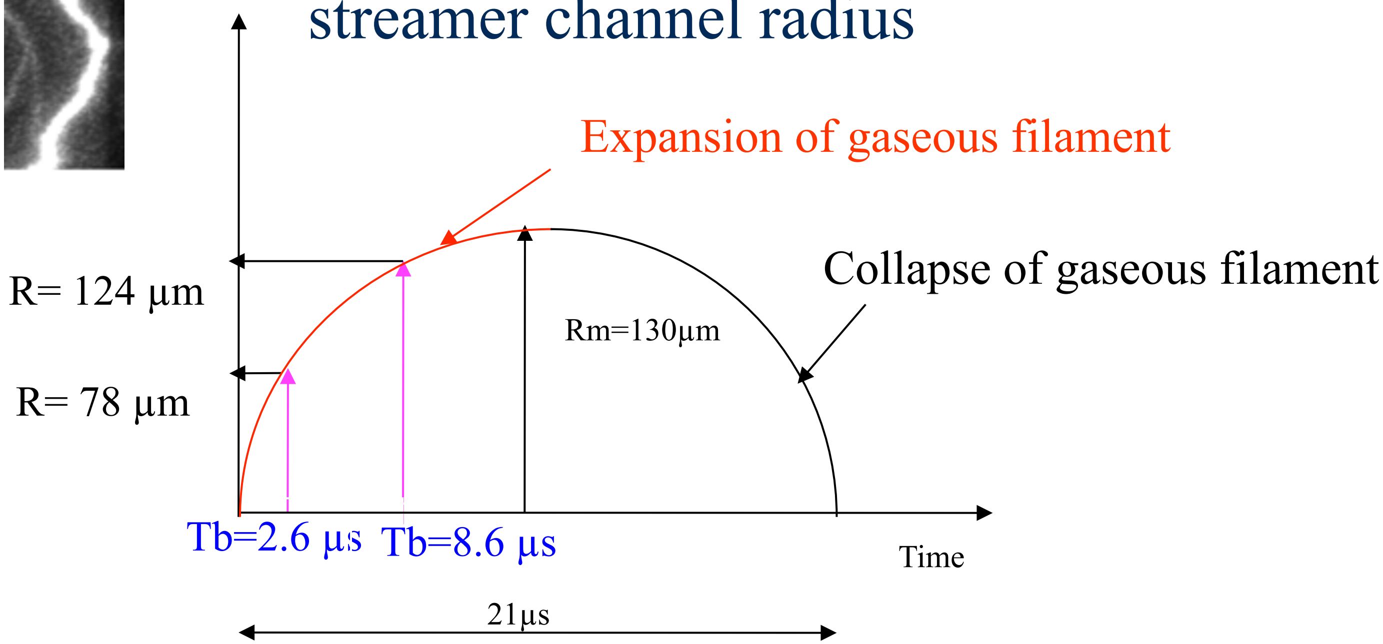

P Gournay and O Lesaint 1994

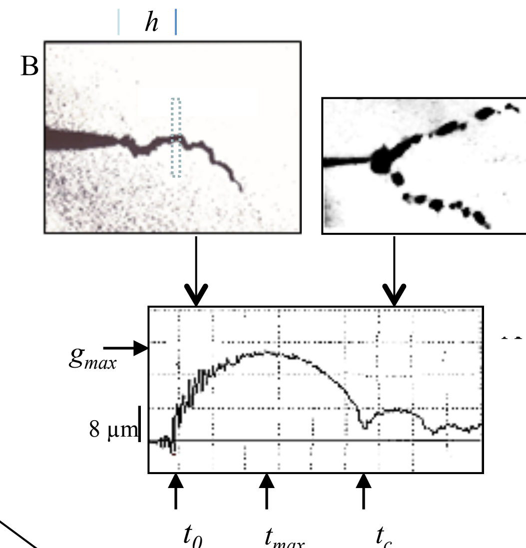

$T_b \nearrow$ The plasma column has expanded $N_g \searrow$

Positive filamentary streamers in liquid nitrogen

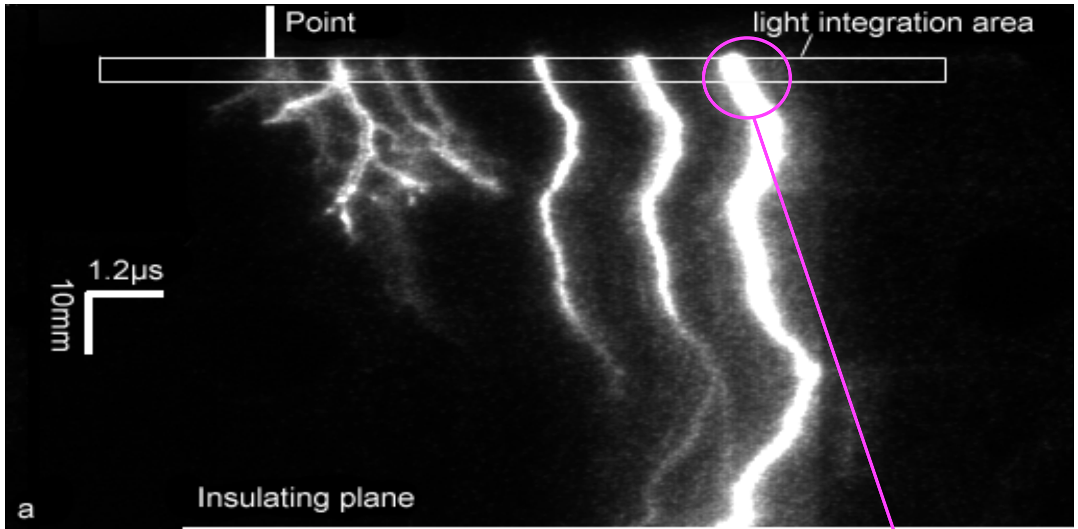

2000 K- 3000 K

Internal Pressure of the gas ~200 B V=30 km/s
Internal Pressure of the gas ~30 B V=10 km/s

N_e=1-5 10^{23} m^{-3}

Spectral analysis of the light emitted from streamers in chlorinated alkane and alkene liquids

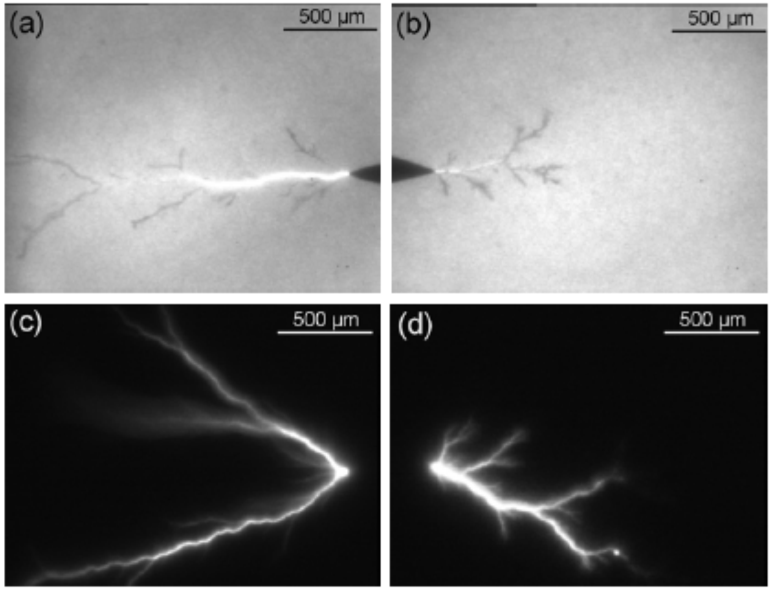

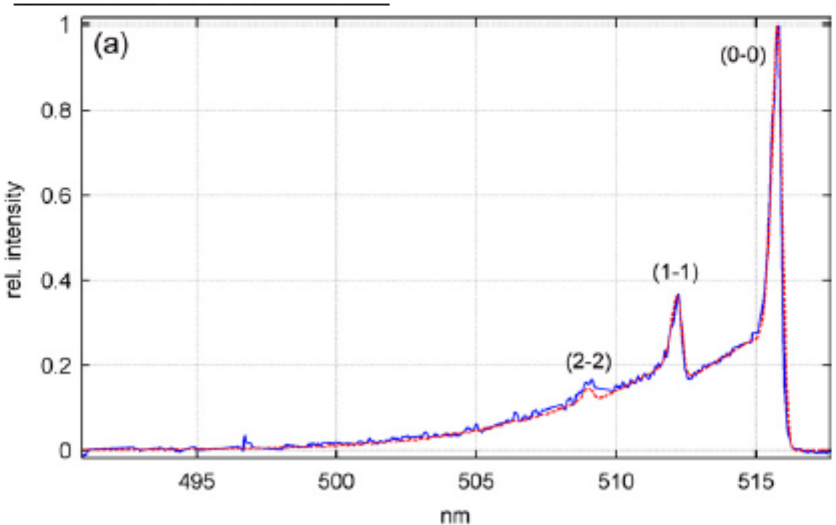

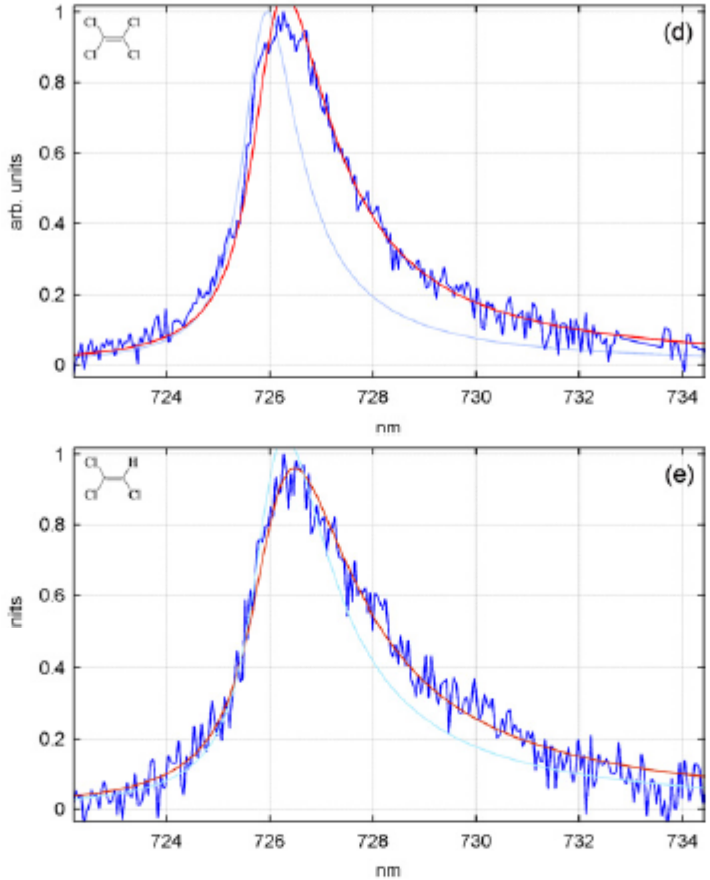

725,6 nm

20-30 km/s

T_{rot} =3000-4000 K

P=86-136 bar

N_e=4-8 10^{23} m^{-3}

Optical Emission from Helium Cryoplasma

Discharge in dense fluids (liquids or high-pressure gases :1-100 bar)

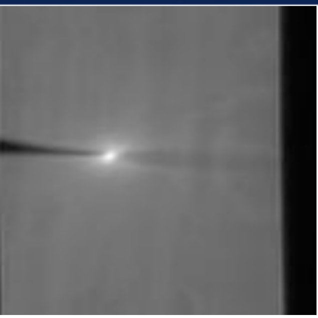

V ~ kV DC, I ~ 0,1-50μA
P=0,1-100mW,
gap distance~5-8 mm
R_{tip} ~ 0,1-2μm

Corona-discharge

Liquid Helium

Gas → liquid

T ↘

Temperature: 300 K → 4.2 K

Density N: $2\ 10^{19}$ cm^{-3} → $2\ 10^{22}$ cm^{-3}

Goal:

Determine N_e, T_e, T, N_{He}

- pure liquid
- intense luminescence
- helium is atomic.
- Low electronic mobility.
- physical and Thermodynamic properties
- interaction potential ab initio He*-He and He_2*- He

Important input parameters for the collision-radiative model in the theoretical study of the corona-discharges

Helium Cryoplasma

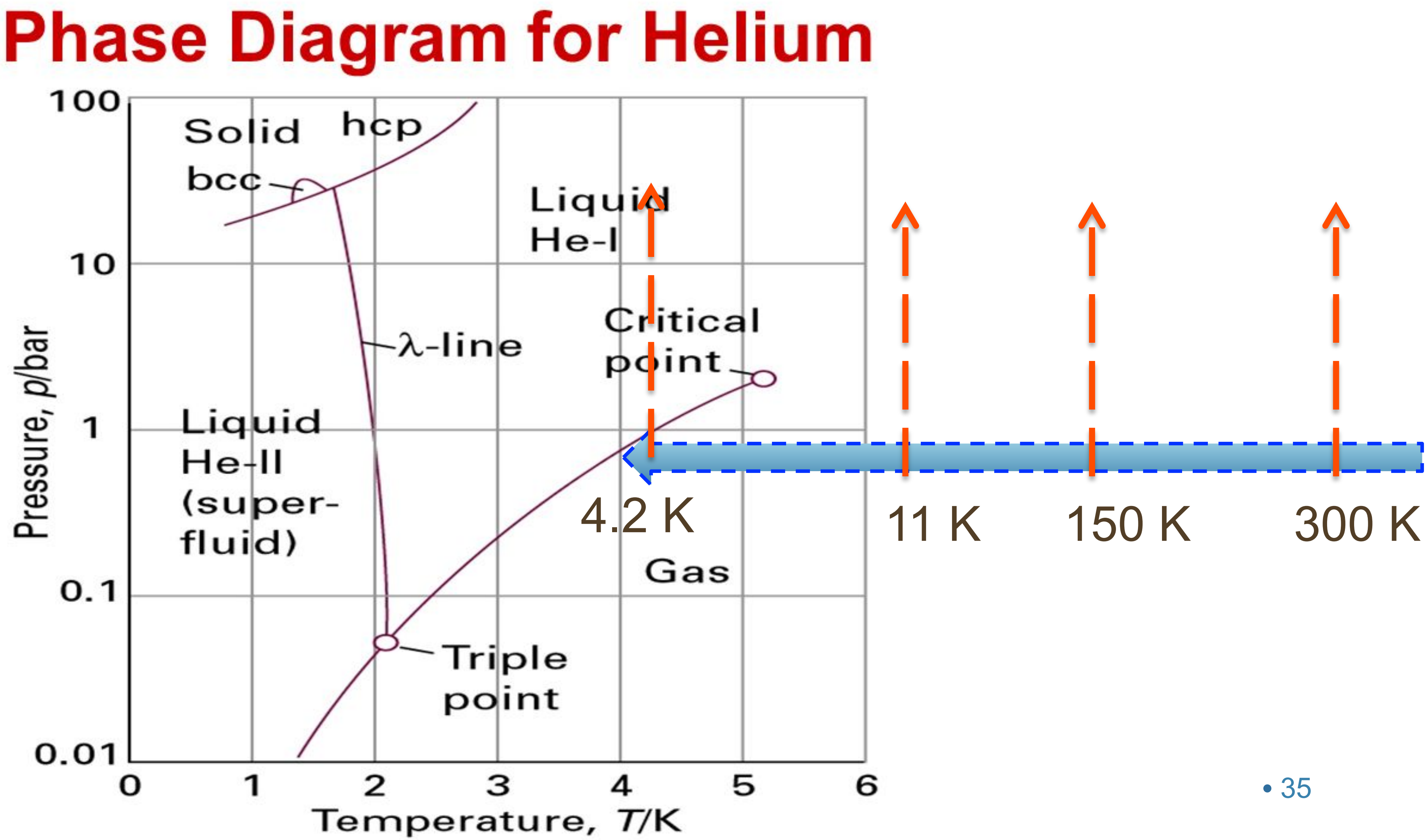

Temperature :
Rotational temperature measurements

300 K (P) — 150 K (P) — 11 K (P) — 4.2 K (P) →

300 K (P)	150 K (P)	11 K (P)	4.2 K (P)
N_2, N_2^+ He_2	N_2, N_2^+ He_2	He_2	He_2

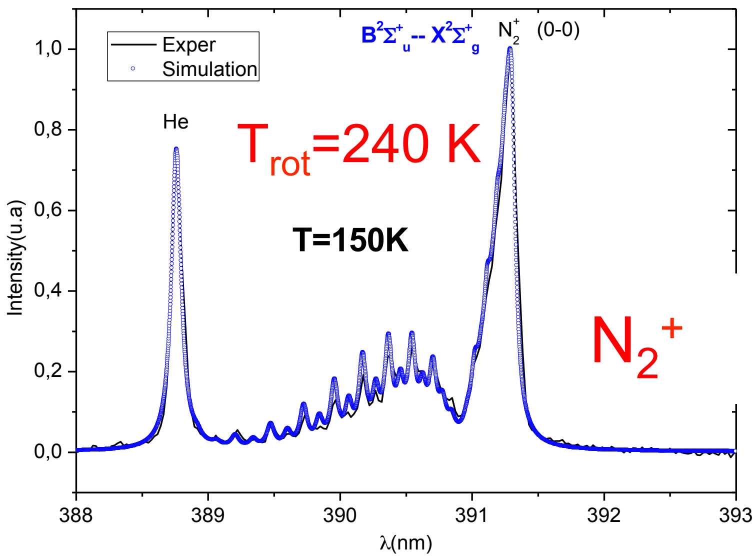

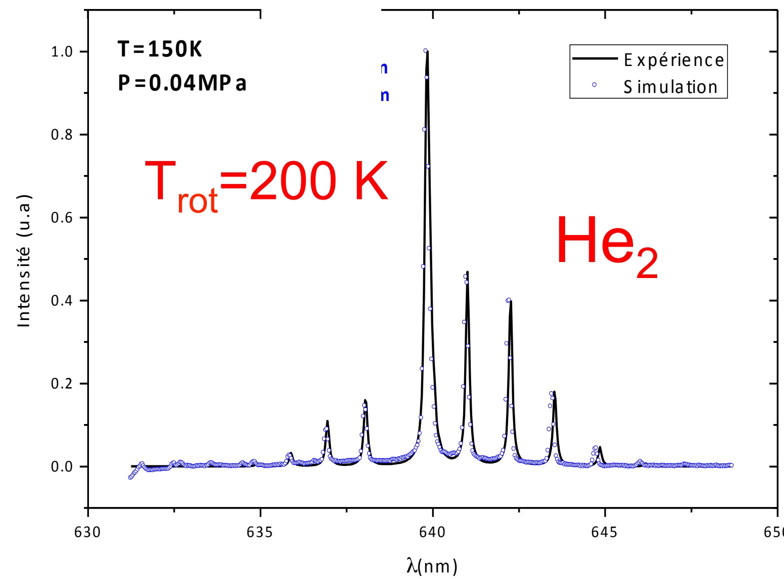

The rotational line of Nitrogen molecular bands was a probe to thermodynamic temperature at non equilibrium plasma.

Temperature :
Rotational temperature measurements

300 K (P)	150 K (P)	11 K (P)	4.2 K
300-500 K	240-280 K	80-240 K	
$T_{rot}= 31\ P + 370$	$T_{rot}= 33\ P + 263$	$T_{rot}= 208\ P + 62$	

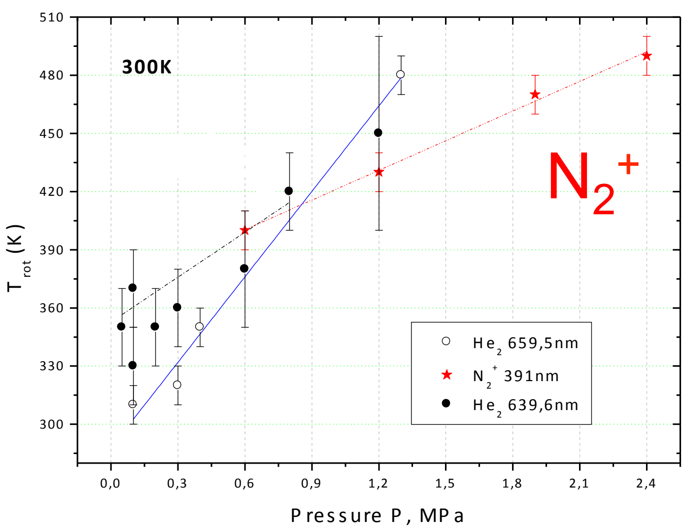

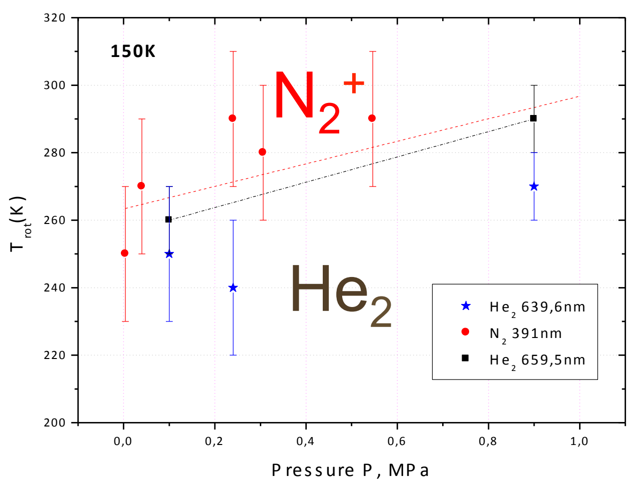

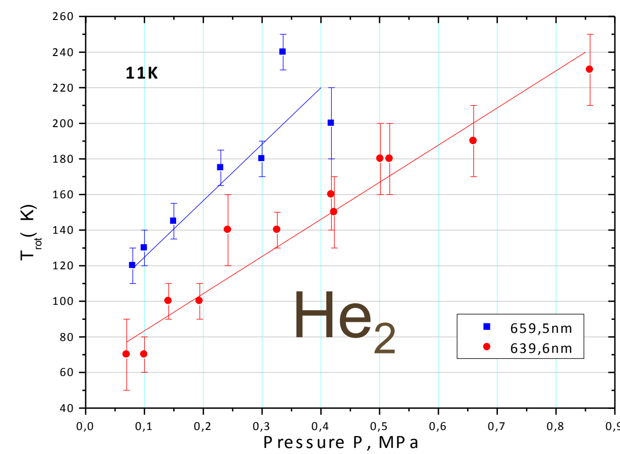

Temperature :
Rotational temperature measurements

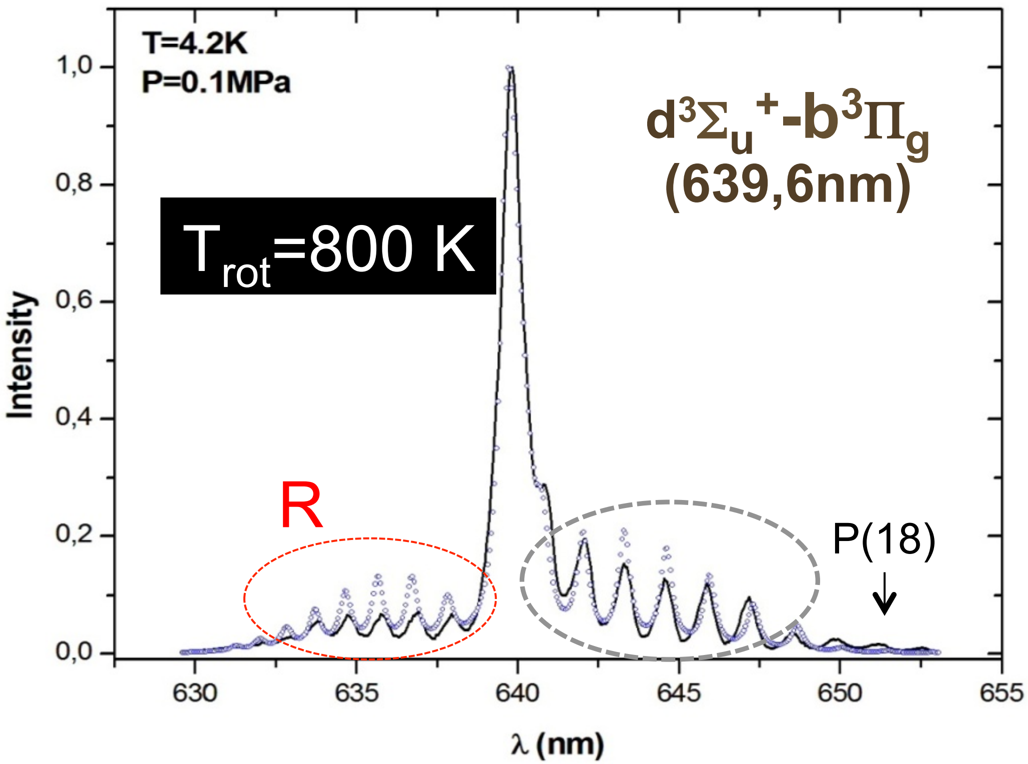

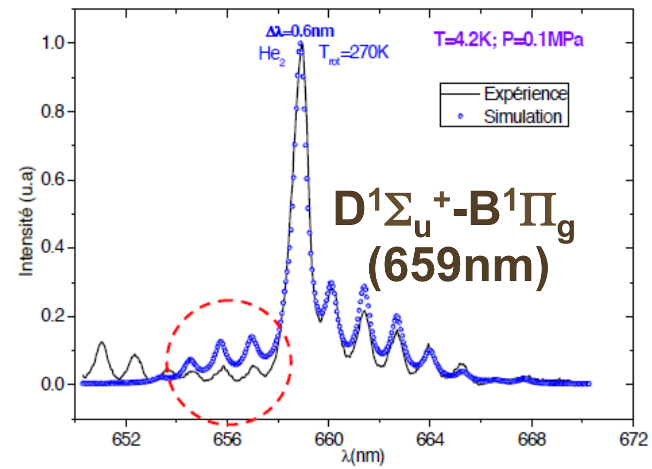

Strongly Blue Shifted

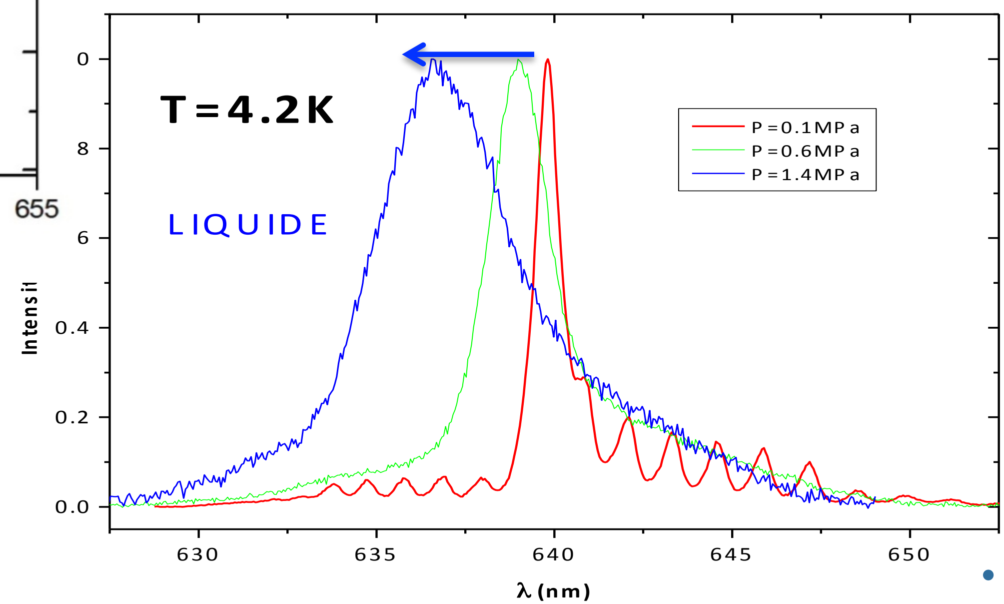

No boltzmann distribution
High degree of rotational excitation

Electron number density : N_e

300 K (P) — 150 K — 11 K — 4.2 K(P)

- Hα : 656 nm
- Hβ : 486 nm
- He I : 492 nm

He 492 nm

300 K

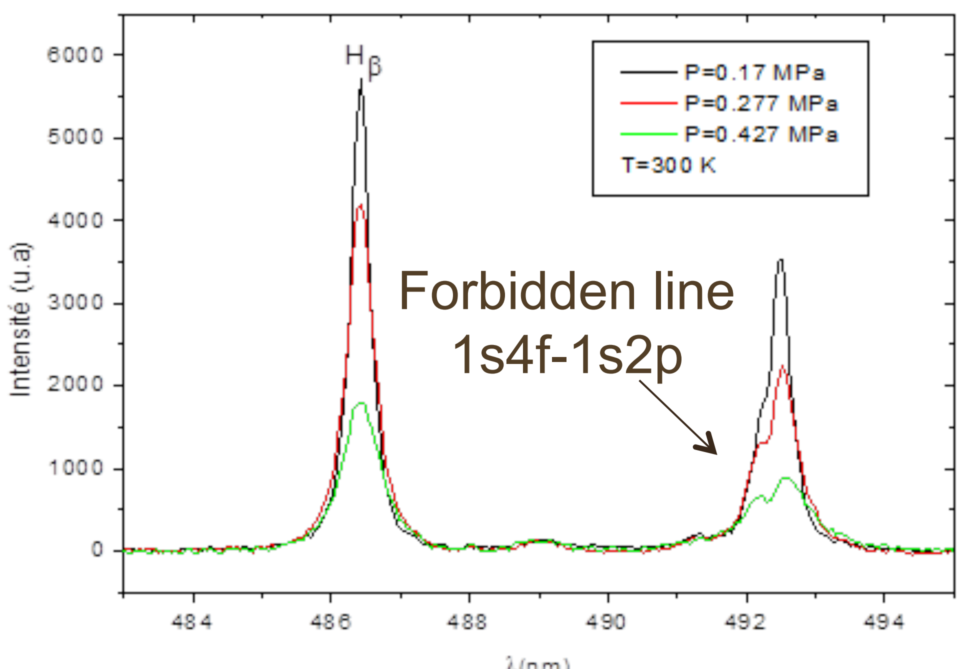

Forbidden line
1s4f-1s2p

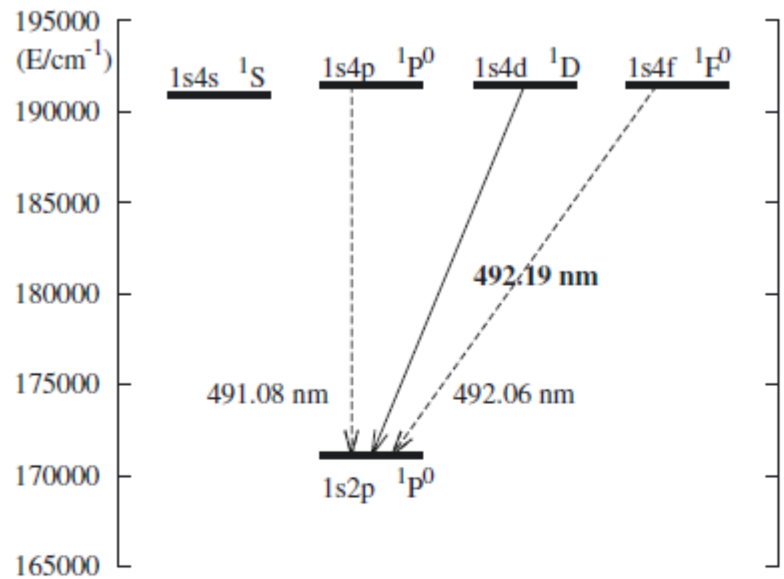

Code comparison code workshops
http://plasma-gate.weizmann.ac.il/slsp/

The 4th Spectral Line Shapes in Plasmas code comparison workshop– Baden – March 20th to 24th, 2017

corona discharge in helium 300 K

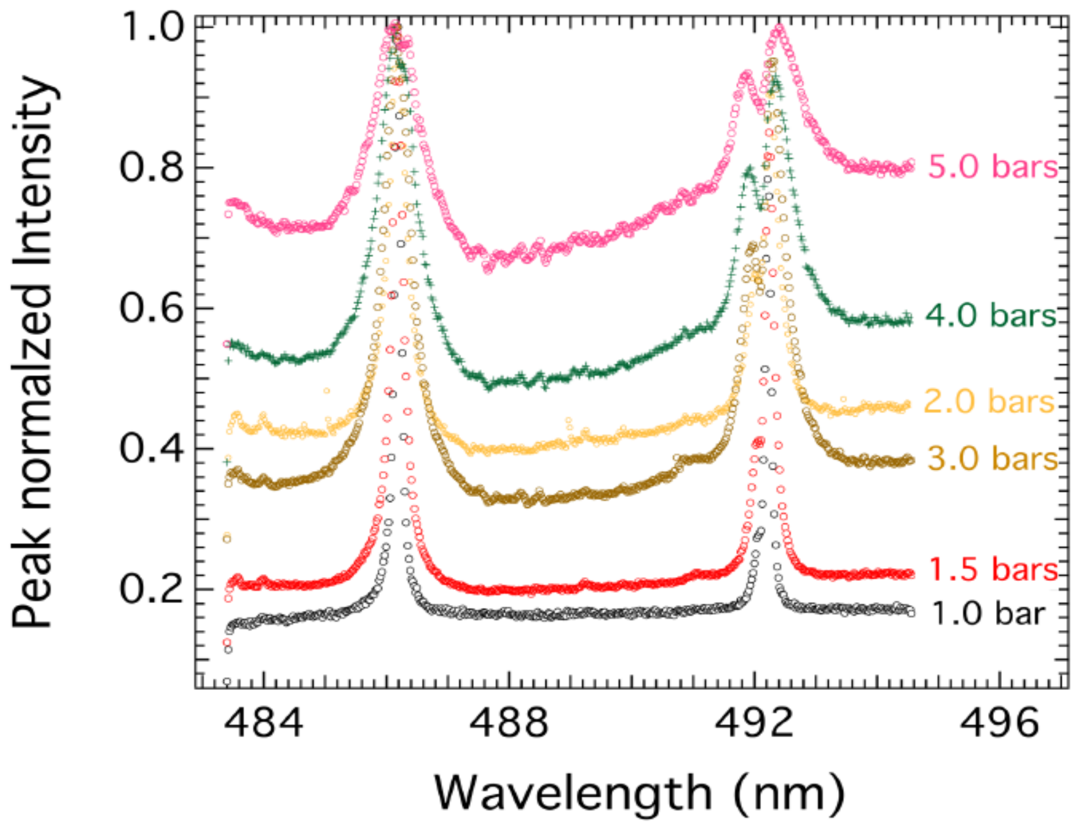

Comparison of the FWHM of the H-β Line

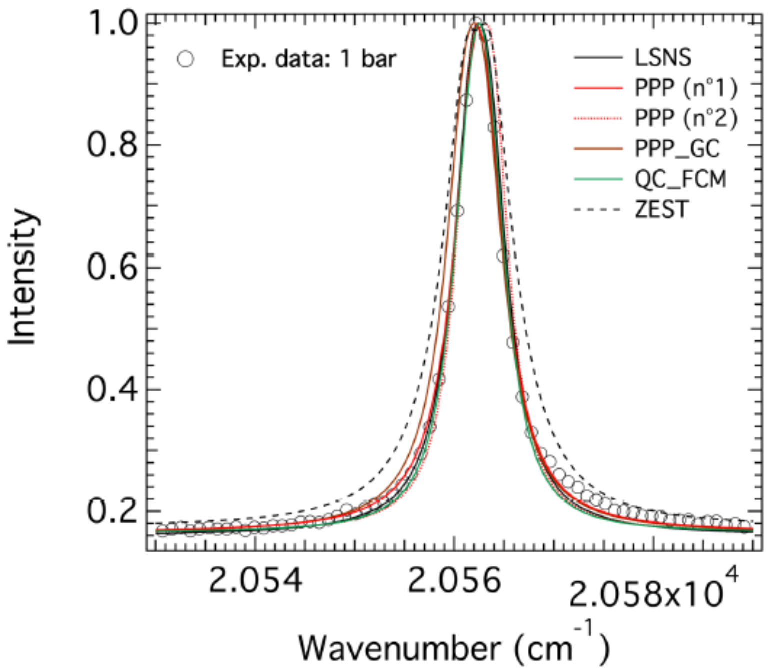

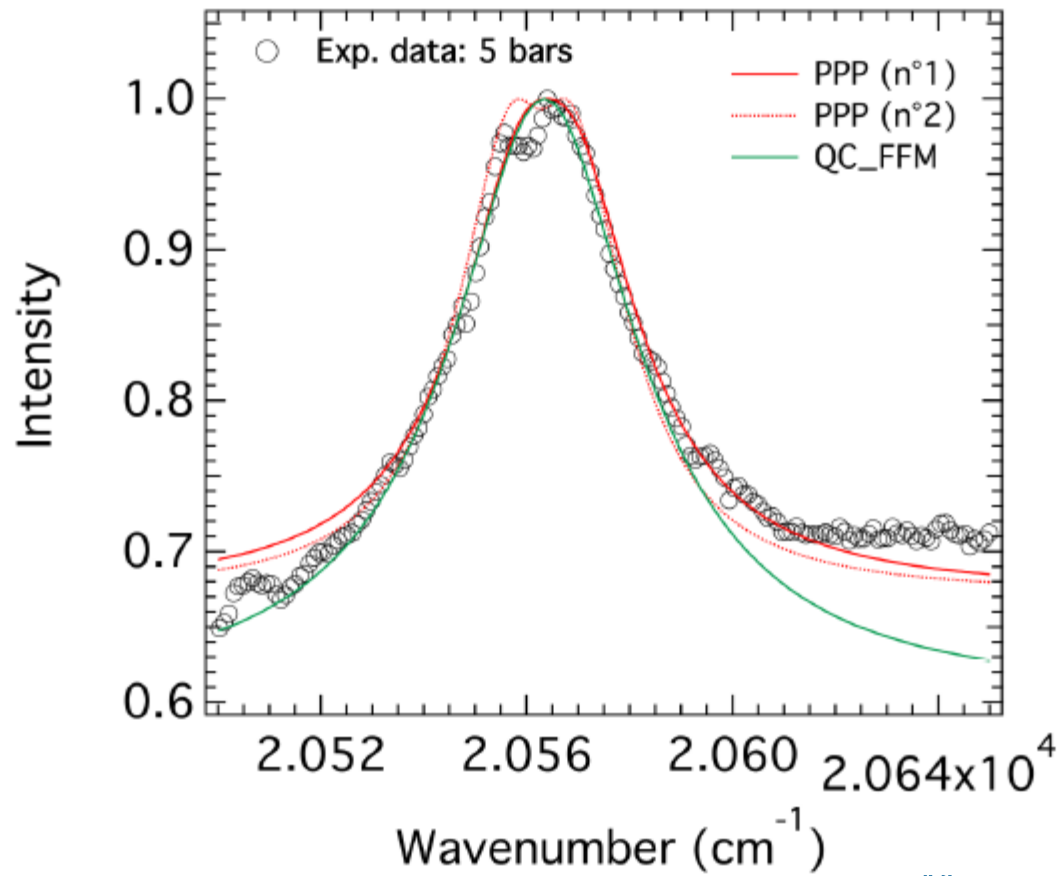

H-β Line in a Corona Helium Plasma: A Multi-Code Line Shape Comparison

Table 3. The electron densities (in units of 10^{15} cm^{-3}) as inferred from the fit of the experimental H-β spectra by the contributing codes. P is the pressure in units of bars.

Case n°	P	LSNS	PPP (n°1)	PPP (n°2)	PPP_GC	QC_FFM	ZEST
1	1	0.5	0.15	0.26	0.18	0.8	1.2
2	1.5	1.1	0.3	0.58	0.38	2.2	2.7
3	2	-	0.55	1.0	1.3	4.7	-
4	3	-	0.9	2.0	-	10.0	-
5	4	-	1.3	2.8	-	15.0	-
6	5	-	1.9	3.8	-	27.0	-

RR Sheeba, M Koubiti, N Bonifaci, F Gilleron, C Mossé… - *Atoms* **2018**, *6*(2), 29; https://doi.org/10.3390/atoms6020029

Broadening of the Neutral Helium 492 nm Line in a Corona Discharge: Code Comparisons

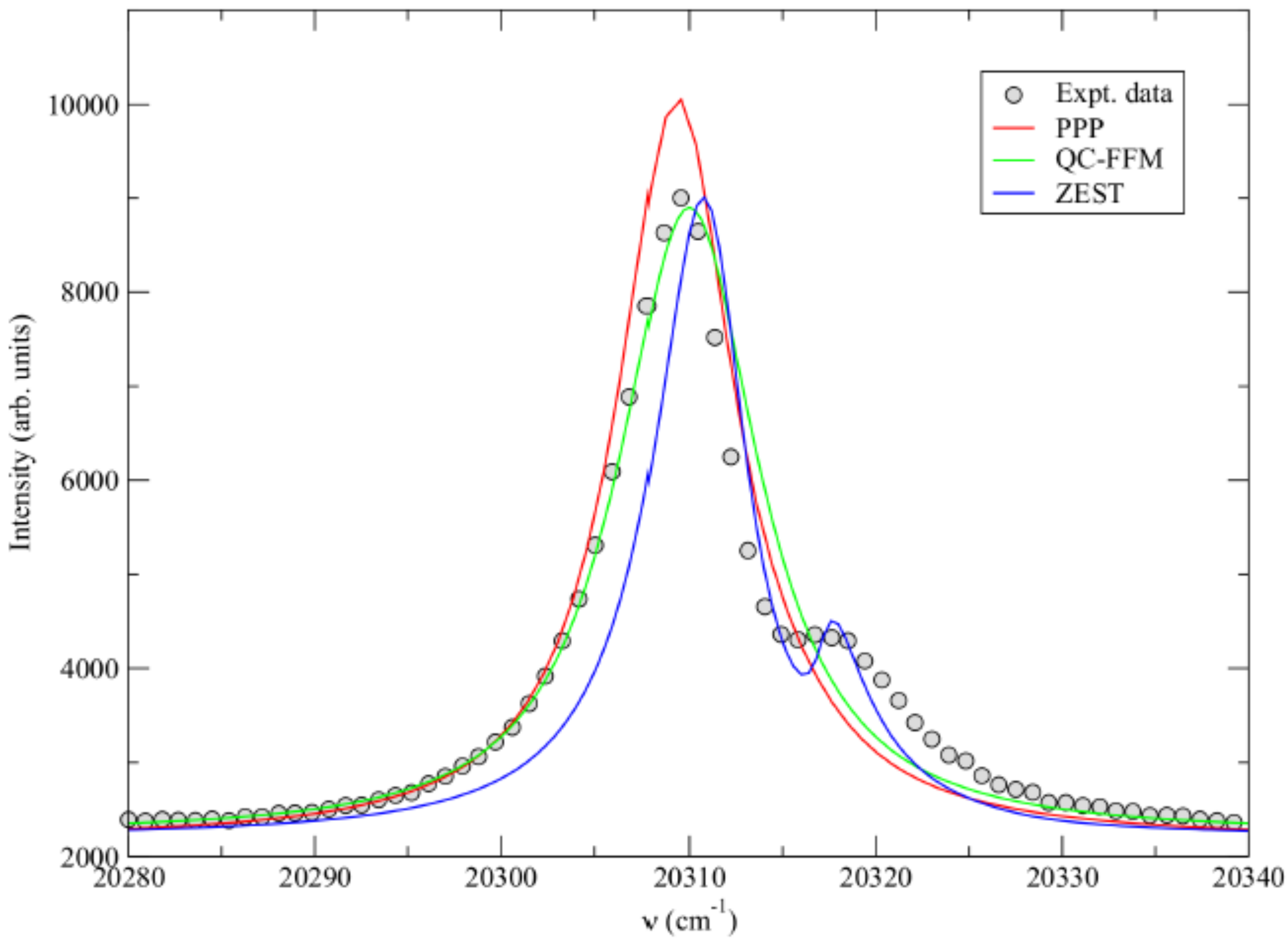

1.5 bar 300 K

RR Sheeba, M Koubiti, N Bonifaci, F Gilleron, JC Pain… **-**
Atoms **2018**, *6*(2), 19; doi: 10.3390/atoms6020019

A New Procedure to Determine the Plasma Parameters from a Genetic Algorithm Coupled with the Spectral Line-Shape Code PPP

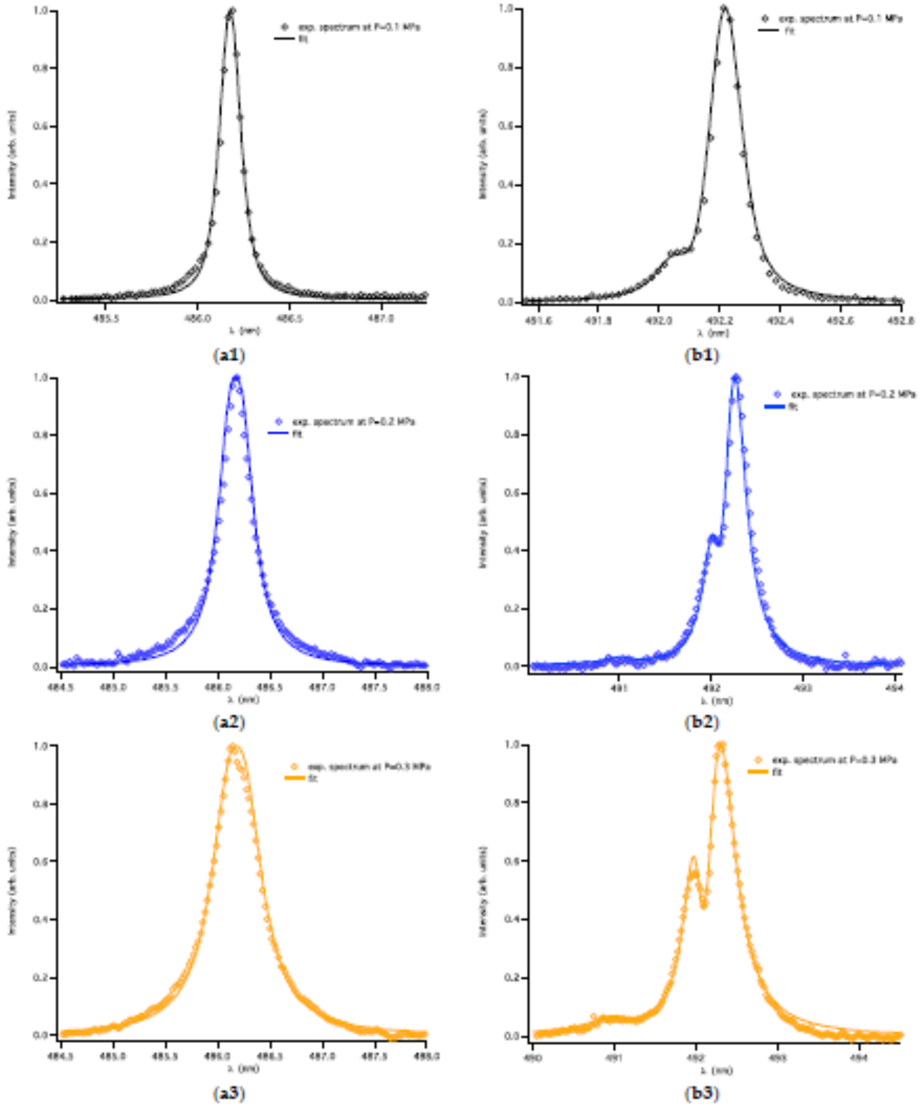

C Mossé, P Génésio, N Bonifaci, A Calisti- *Atoms* **2018**, ***6*(4), 55;**
https://doi.org/10.3390/atoms6040055

A New Procedure to Determine the Plasma Parameters from a Genetic Algorithm Coupled with the Spectral Line-Shape Code PPP

Table 5. Results of the fitting GA analysis of the H-β line. n_e: electron density; T_e: electron temperature; $\Delta\lambda_{VDW}$: van der Waals width; $\Delta\lambda_{ins}$: Gaussian width.

Pressure (bar)	n_e (cm^{-3})	T_e (10^4 K)	$\Delta\lambda_{VDW}$ (nm)	$\Delta\lambda_{ins}$ (nm)
1	10^{14}	1.23	7.2×10^{-2}	8.0×10^{-2}
2	8×10^{14}	1.17	15.2×10^{-2}	8.0×10^{-2}
3	1.85×10^{15}	1.21	24.2×10^{-2}	8.0×10^{-2}

Table 6. Results of the fitting GA analysis of the He I 492 nm line.

Pressure (bar)	n_e (cm^{-3})	T_e (10^4 K)	$\Delta\lambda_{VDW}$ (nm)	$\Delta\lambda_{ins}$ (nm)
1	10^{15}	1.21	2.93×10^{-2}	8.0×10^{-2}
2	3.96×10^{15}	1.16	5.82×10^{-2}	8.0×10^{-2}
3	8×10^{15}	1.16	9.7×10^{-3}	8.0×10^{-2}

Electron number density : N_e 492 nm

Computer simulation method

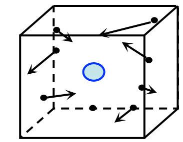

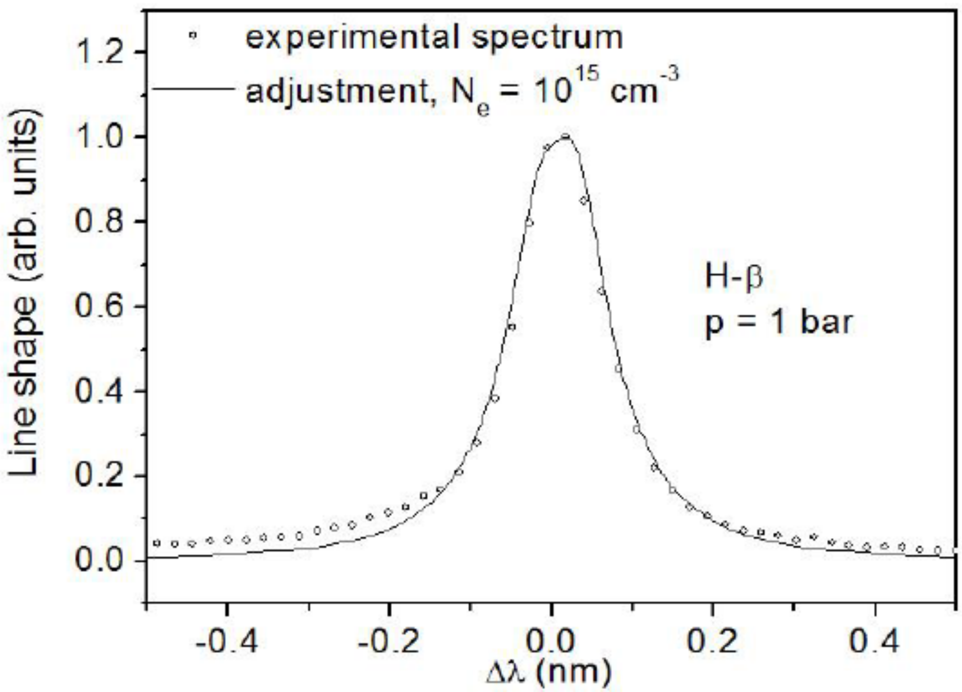

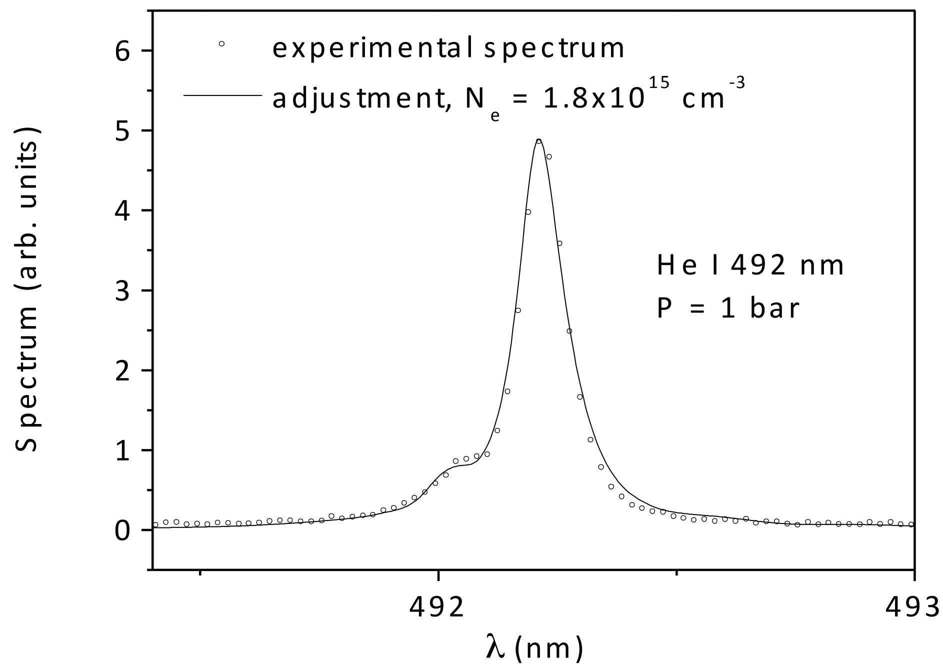

$T_e = 10^4$ K

Line Shape Modeling for the Diagnostic of the Electron Density in a Corona Discharge

J Rosato, N Bonifaci, Z Li, R Stamm - **Atoms**, 2017

Electron number density : N_e

300 K (1-10 bar)

4.2 K (P)

10^{15}-10^{16} cm^{-3}

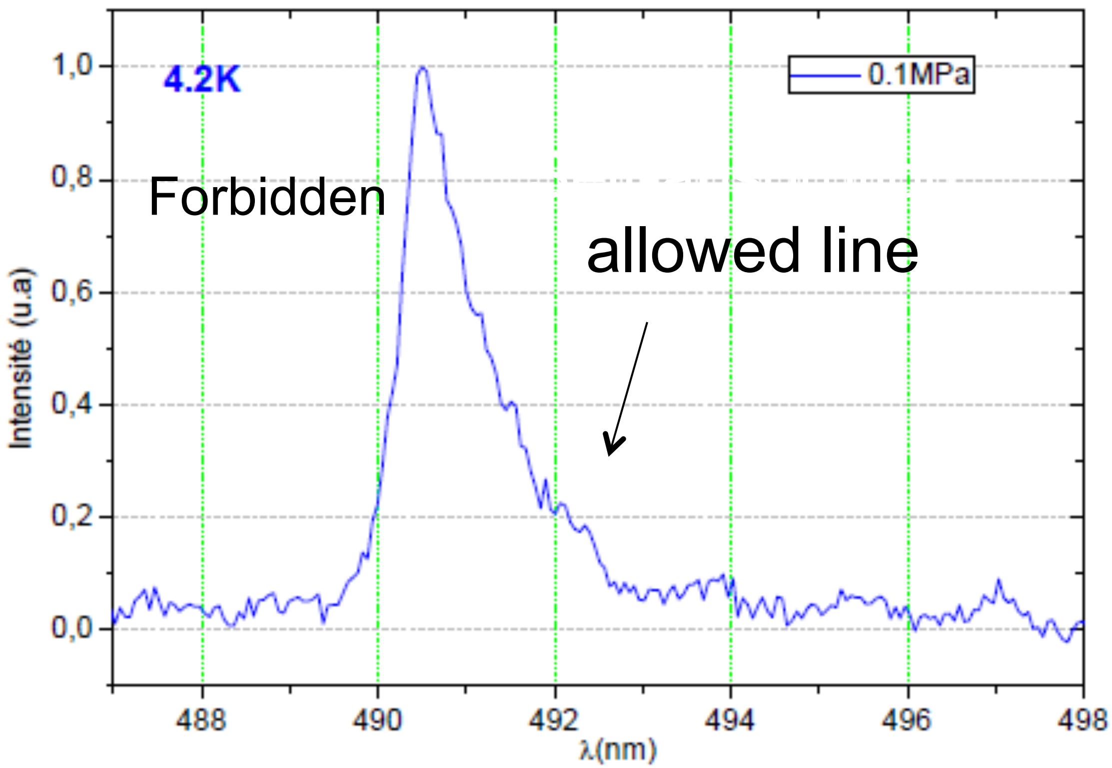

Neutral Perturbers Density : N_{He}

300 K (P) → 4.2 K

706 nm (^3S-^3P)

706 nm (^3S-^3P)

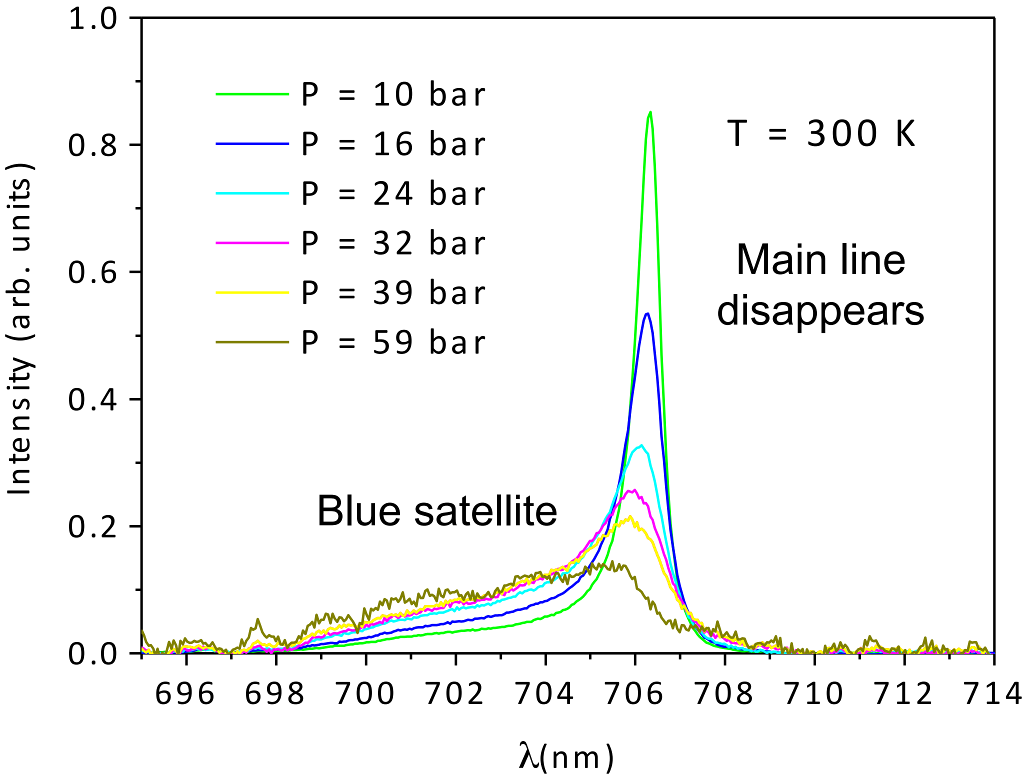

Fourier Transform of the dipole autocorrelation function

$$\phi(\tau) = e^{\left(-N_{He}\, g_{\alpha}(s)\right)}$$

$$g_\alpha(s) = \frac{1}{\sum_{e,e'}{}^{(\alpha)} |d_{ee'}|^2} \sum_{e,e'}{}^{(\alpha)} \int_0^{+\infty} 2\pi\rho\, d\rho \int_{-\infty}^{+\infty} dx\, \tilde{d}_{ee'}[R(0)] \left[e^{\frac{i}{\hbar}\int_0^s dt\, V_{e'e}[R(t)]}\, \tilde{d}^*{}_{ee'}[R(s)] - \tilde{d}_{ee'}[R(0)] \right]$$

Neutral Perturbers Density : N_{He}

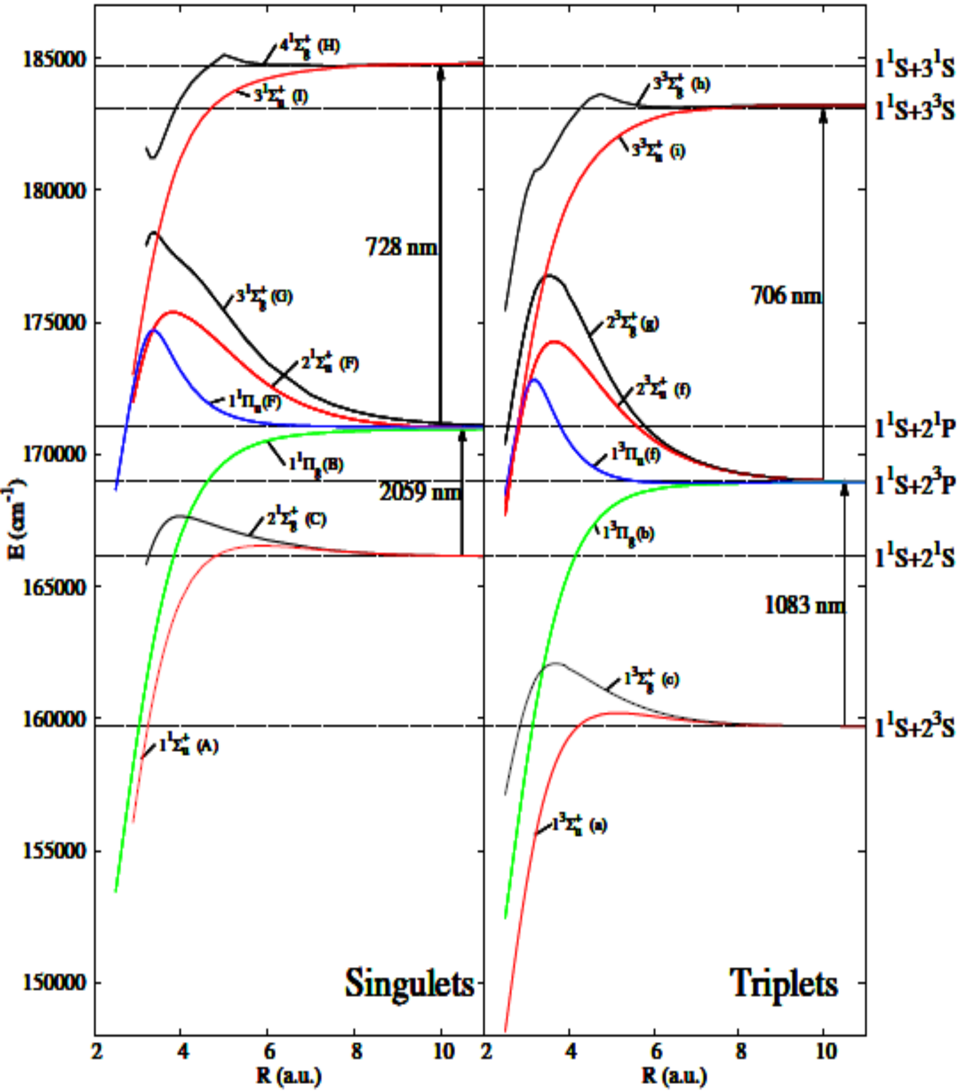

He*-He Potential

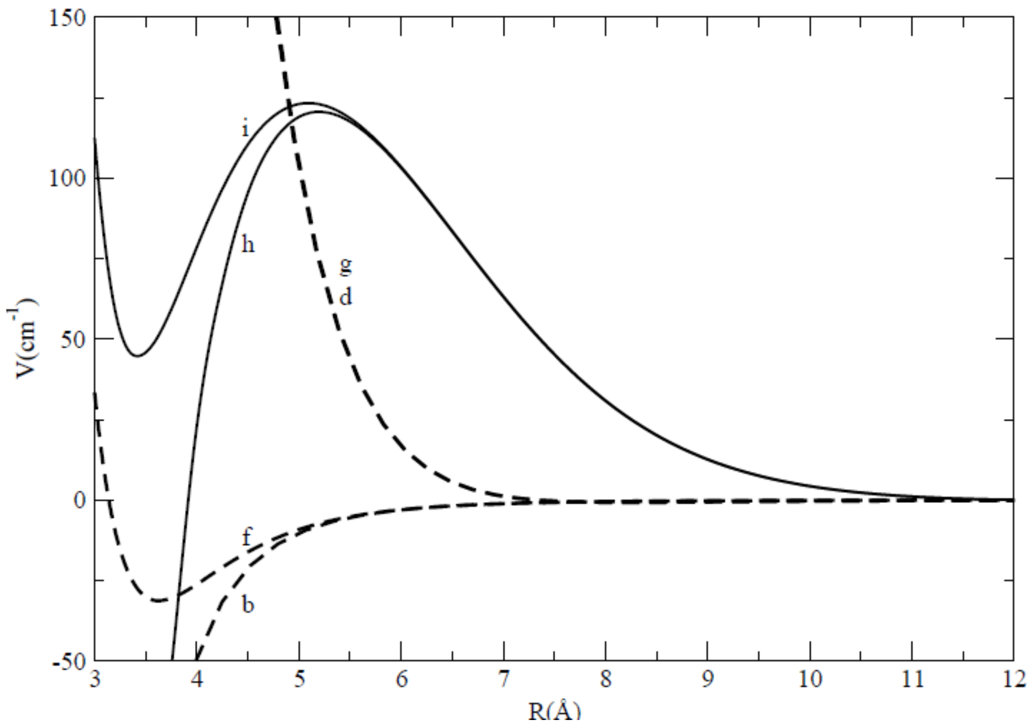

Neutral Perturbers Density : N_{He}

Comparison between experiment and theory

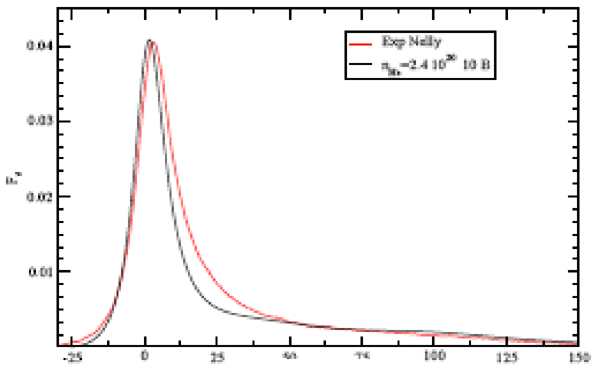

ω (cm^{-1})

N=2.4 10^{20} cm^3

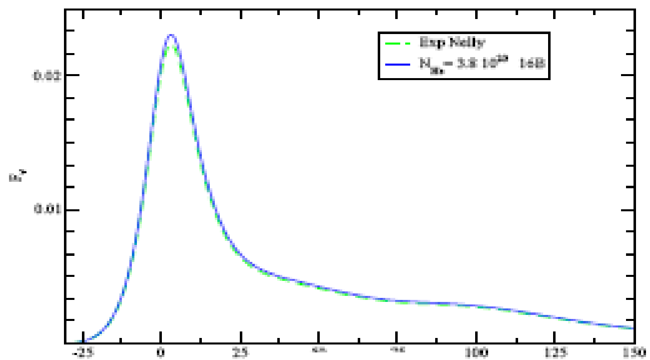

ω (cm^{-1})

N=3.8 10^{20} cm^3

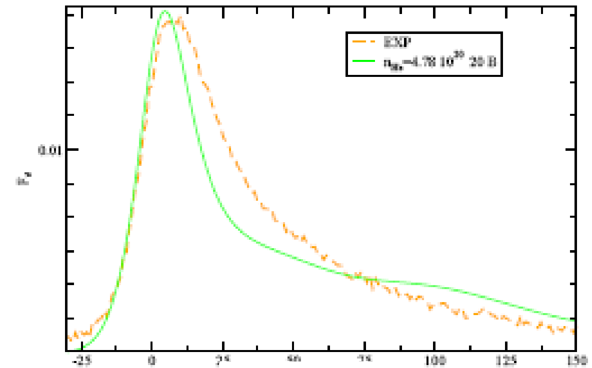

ω (cm^{-1})

N=4.8 10^{20} cm^3

The agreement for a pressure of 1 and 16 Bar is excellent

N ALLARD, et al EPL 88 (2009) 53002

N ALLARD, et al EPJ D 61 (2011) 365-372

Results for He line 706 nm (^3S-^3P) at 300 K

Neutral Perturbers Density : N_{He}

300 K (P)
706 nm

Comparison between experiment and theory

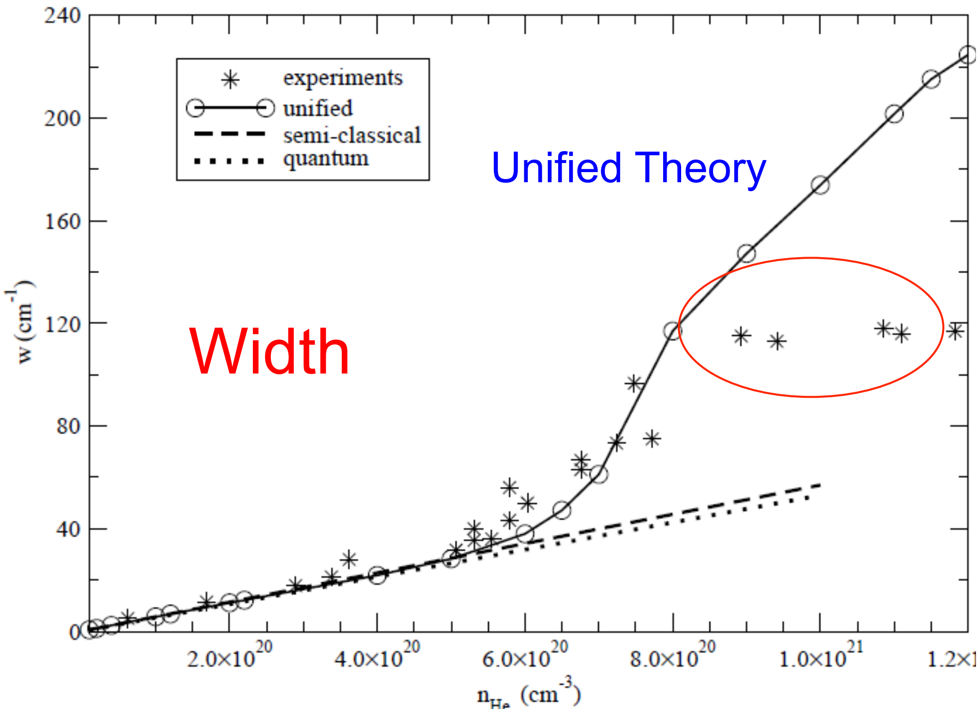

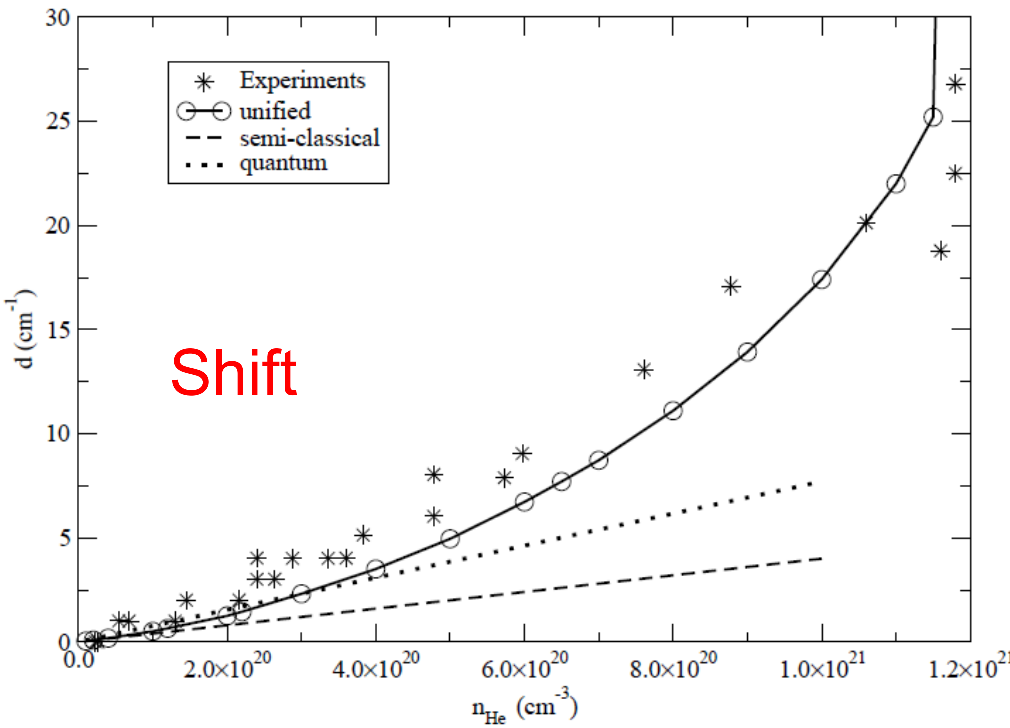

Discrepancy observed at high pressures

Neutral Perturbers Density : N_{He}

Computer simulation method

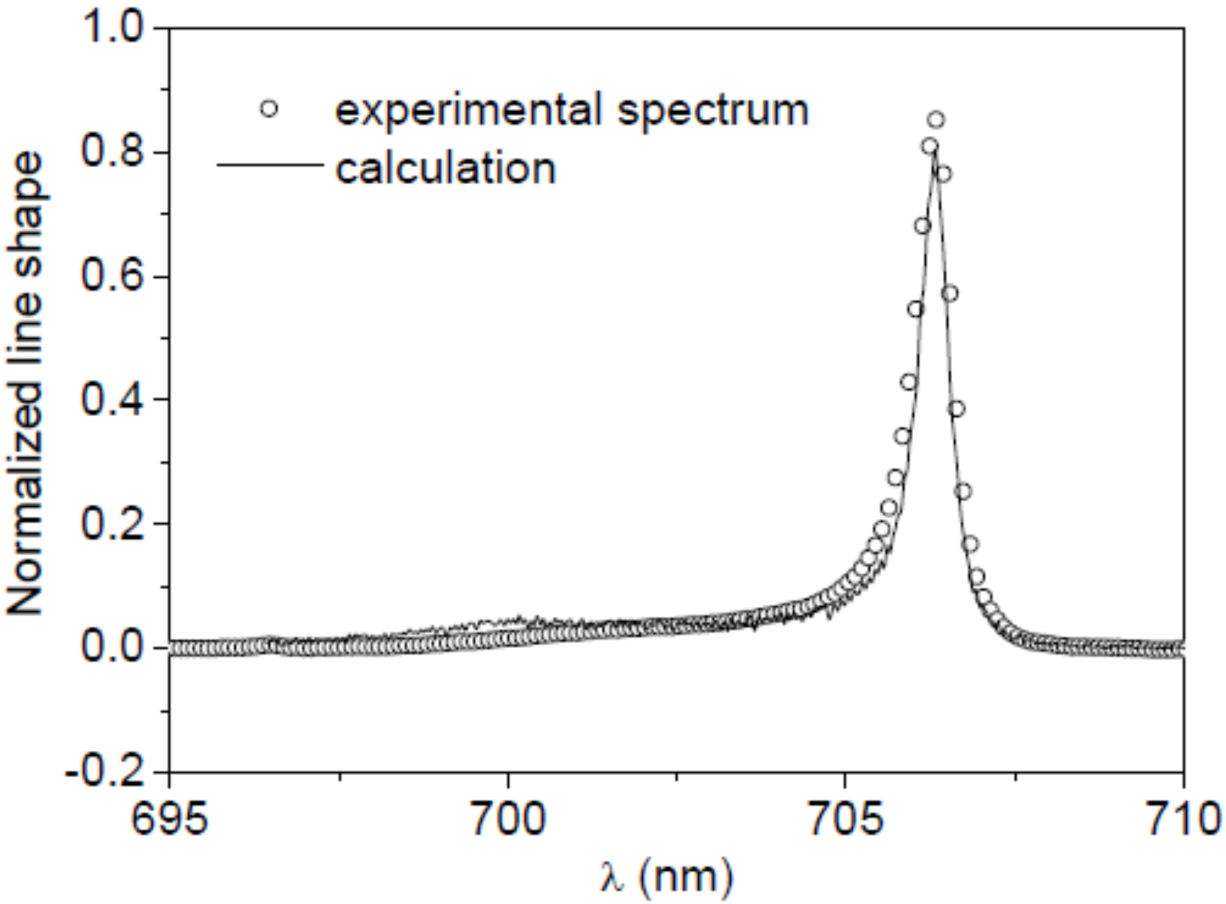

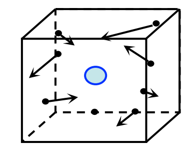

Neutral Perturbers Density : N_{He}

4.2 K

706 nm

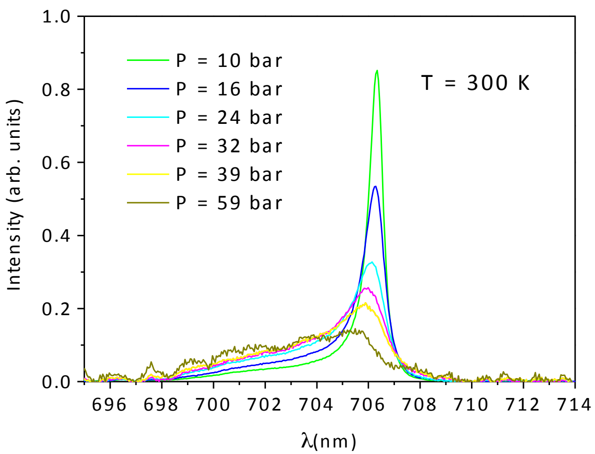

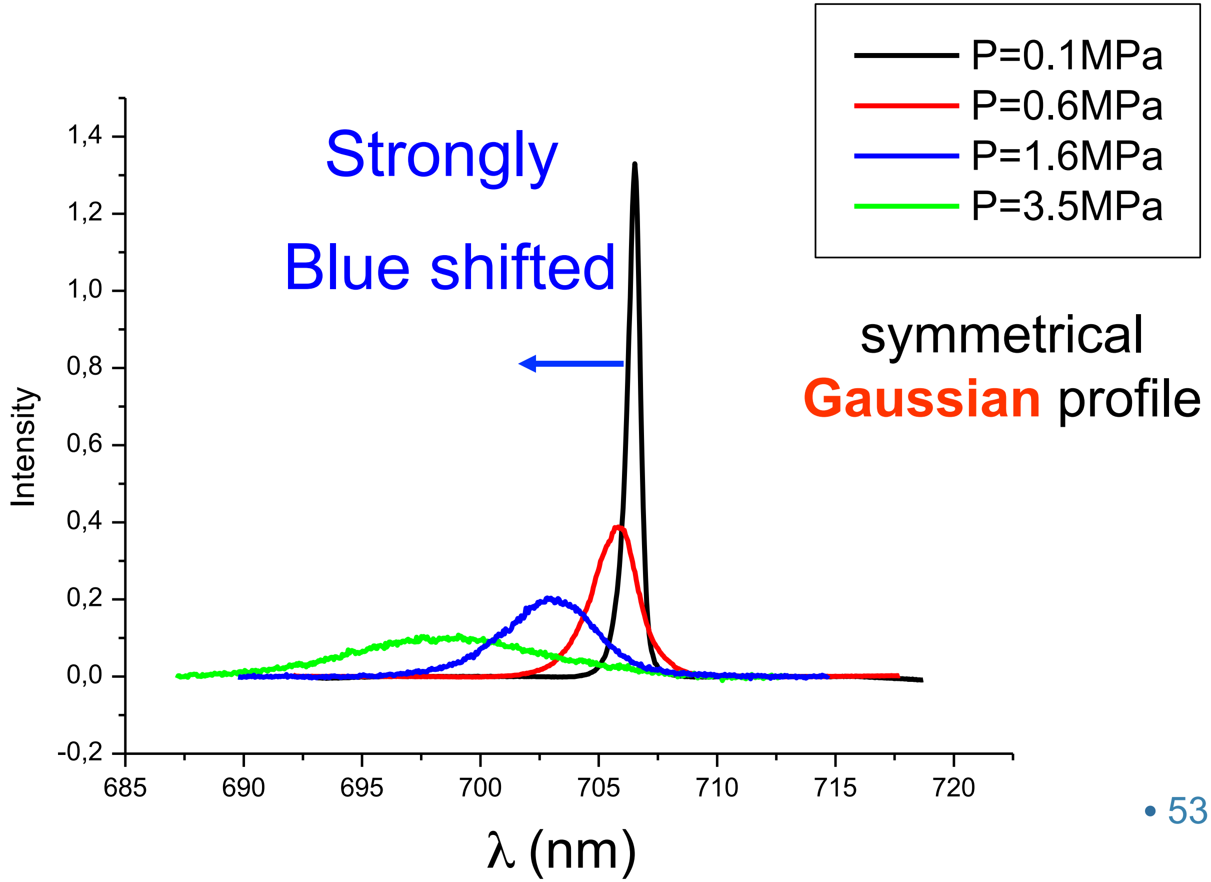

symmetrical
Gaussian profile

Neutral Perturbers Density : N_{He}

Unified semiclassical theory

4. 2 K
706 nm

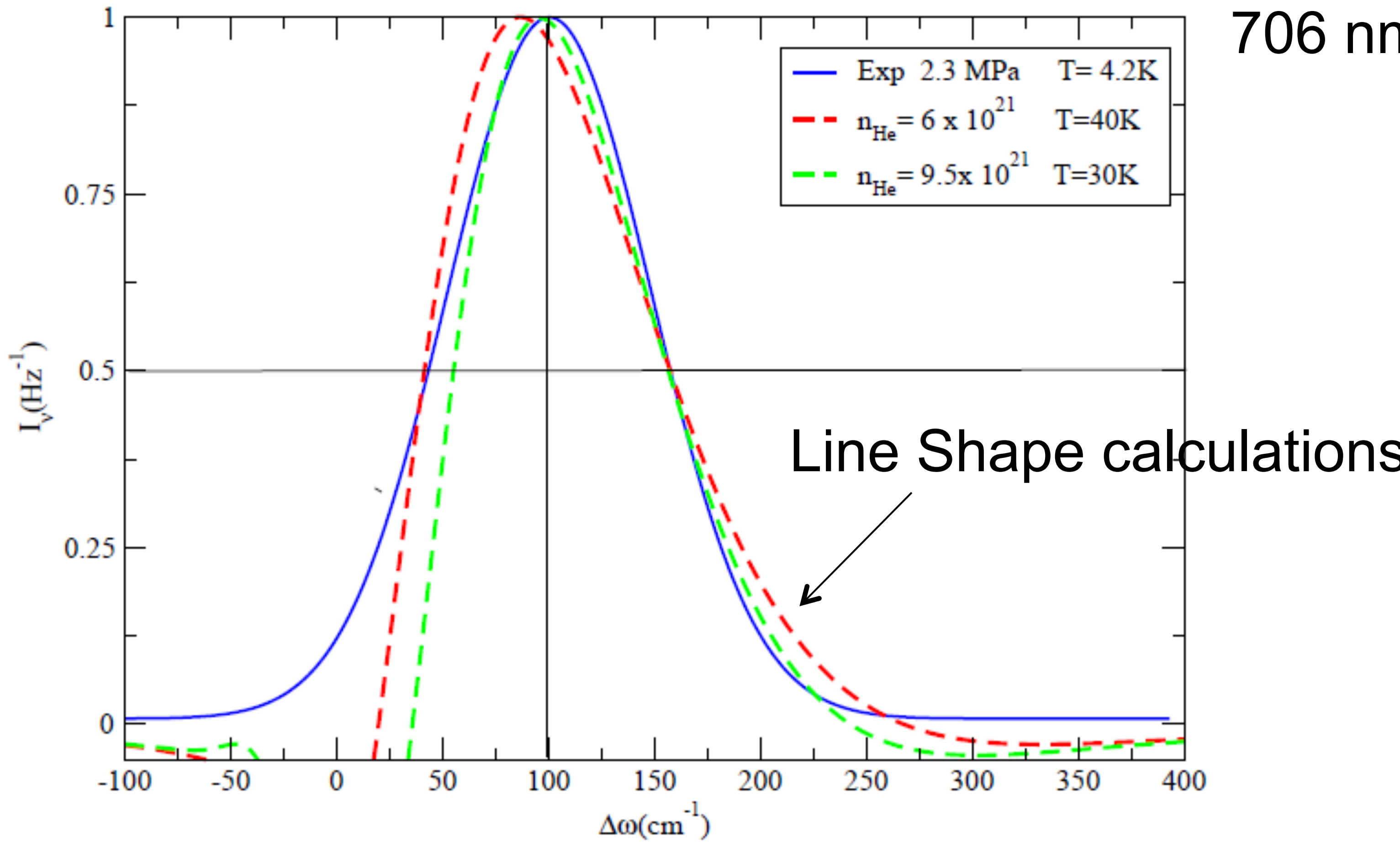

Allard, N. F. 2012, J. Phys. Conf. Ser., 397, 012065

Interpretation ? 4.2 K

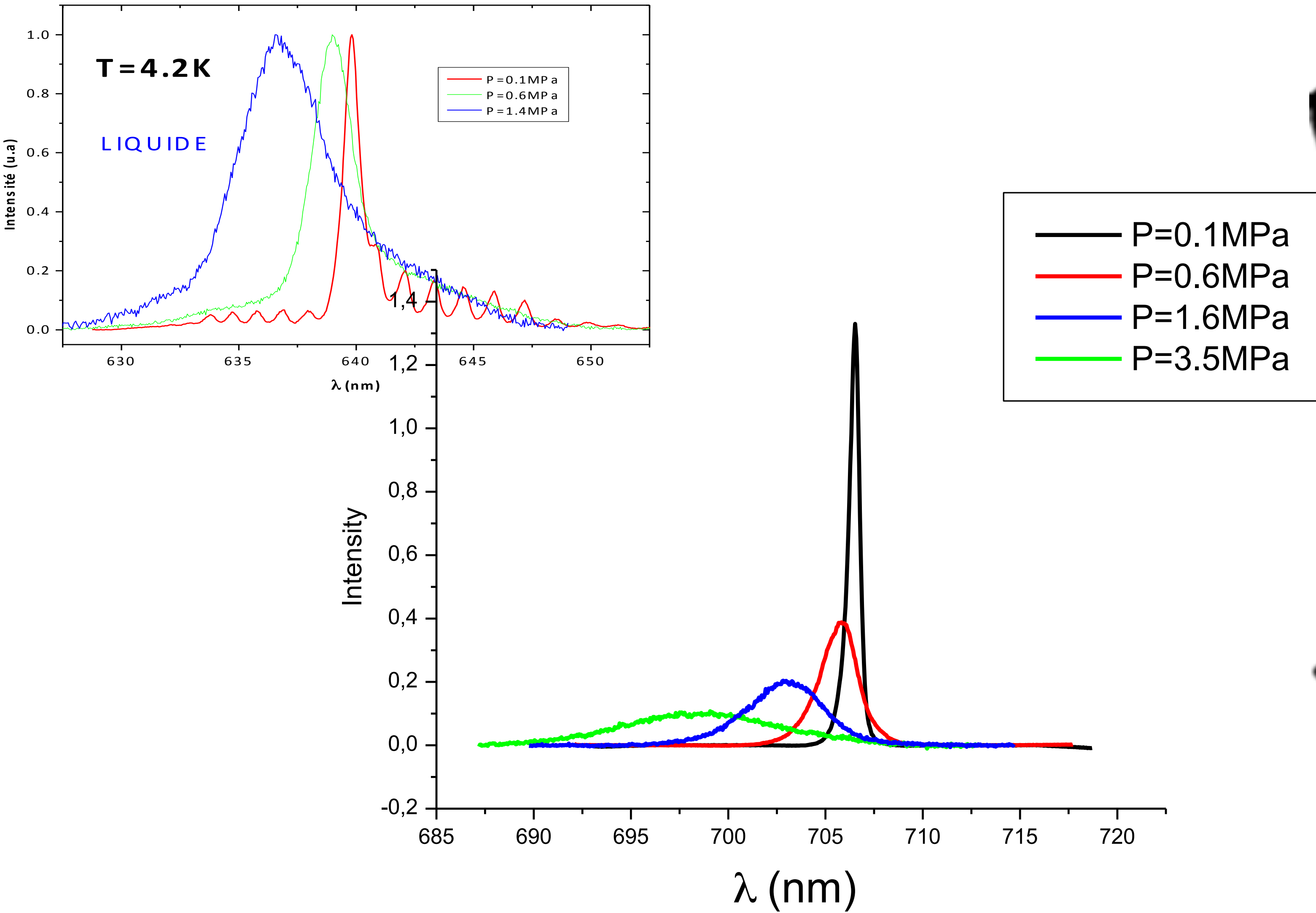

Electron bubbles in liquid ^{4}He

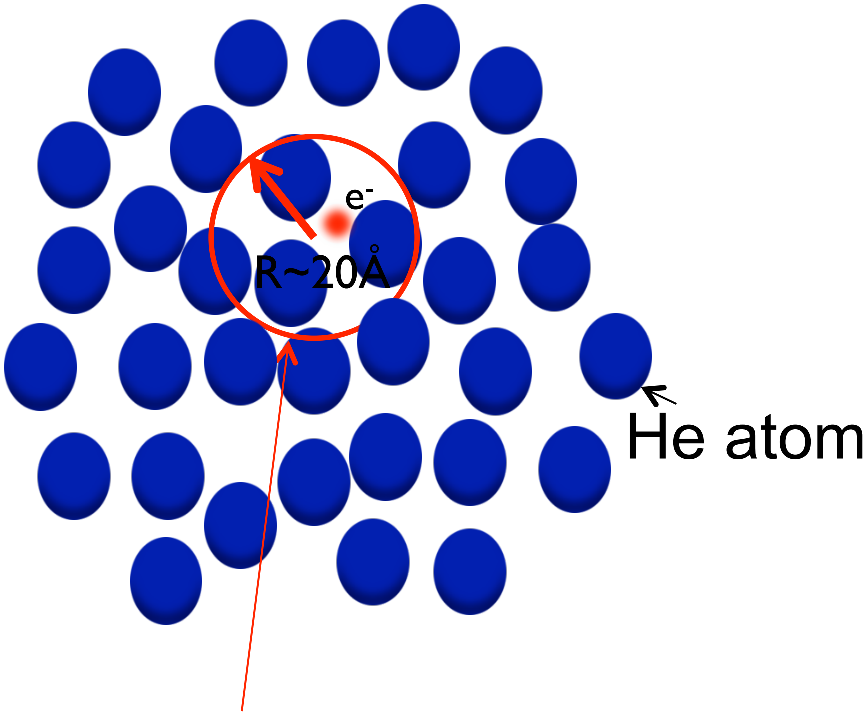

Microscopic cavity: « Bubble »

The mobility decreases rapidly when transitioning from the gas to the liquid phase

The repulsive interaction occurring between e^- and helium atoms.

He localizes electrons in «bubbles»

R_e ~20 Å P=0.1 MPa T= 4.2 K

$$E_{tot} = E_{el} + \underbrace{4\pi R^2 \sigma}_{\text{surface energy}} + \underbrace{\frac{4}{3}\pi R^3 P}_{\text{PV energy}}$$

L He is characterized by its density and surface tension parameter

P is the He pressure

Atomic–bubble model

Schematic model of a Cs atom inside a spherical He bubble.

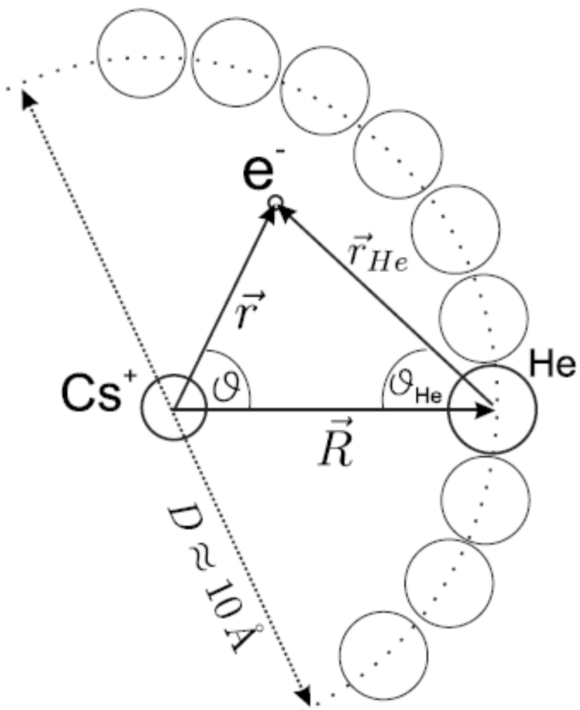

A. Hofer, P. Moroshkin, S. Ulzega, D. Nettels, R. Müller-Siebert, and A. Weis, Phys. Rev. A 76 , 022502 (2007)

Alkali-metal atoms implanted in condensed He reside in nanosize spherical cavities

These bubbles are formed around each impurity atom due to the Pauli principle that forbids any overlap between the closed *S* shells of He atoms and the valence electron of the impurity

$$R_{alkali} \sim 5\text{–}7\ \text{Å}$$

He* He_2* Rydberg electron

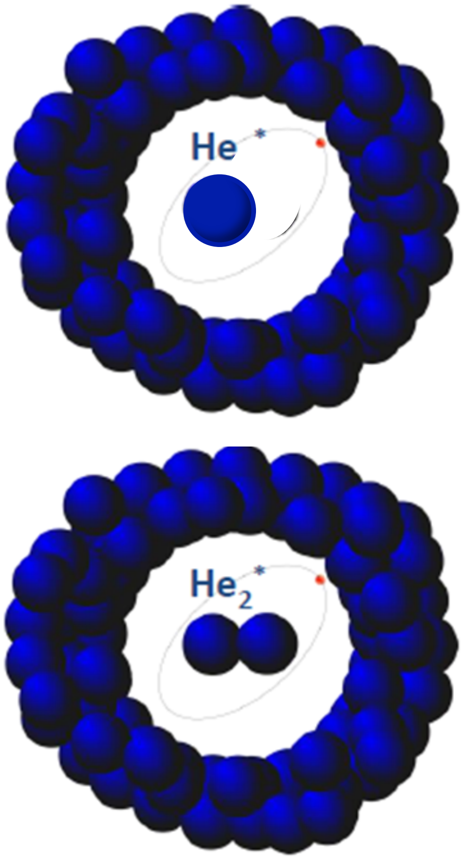

Interpretation:

Microscopic void around
the He*3s and He_2*3d

?

Repulsion between Rydberg e^- and surrounding atoms in the ground state forms bubble

New autocorrelation function with « bath » interaction

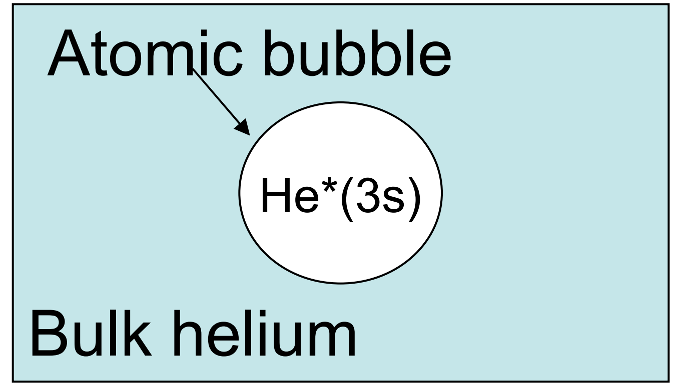

$$\Phi(\tau) = \exp\left(-\int \left(1 - e^{-i\Delta V_{fi}(r)t/\hbar} \right) \rho_i(r)\, d^3 r \right)$$

Difference pair potential between the states corresponding to the emission line

Molpro code

Liquid density in the electronic ground state around 3s calculated using Bosonic Density Functional Theory DFT

Liquid density around He*(3s^{3}S)

Liquid density around 3s^{3}S calculated using DFT

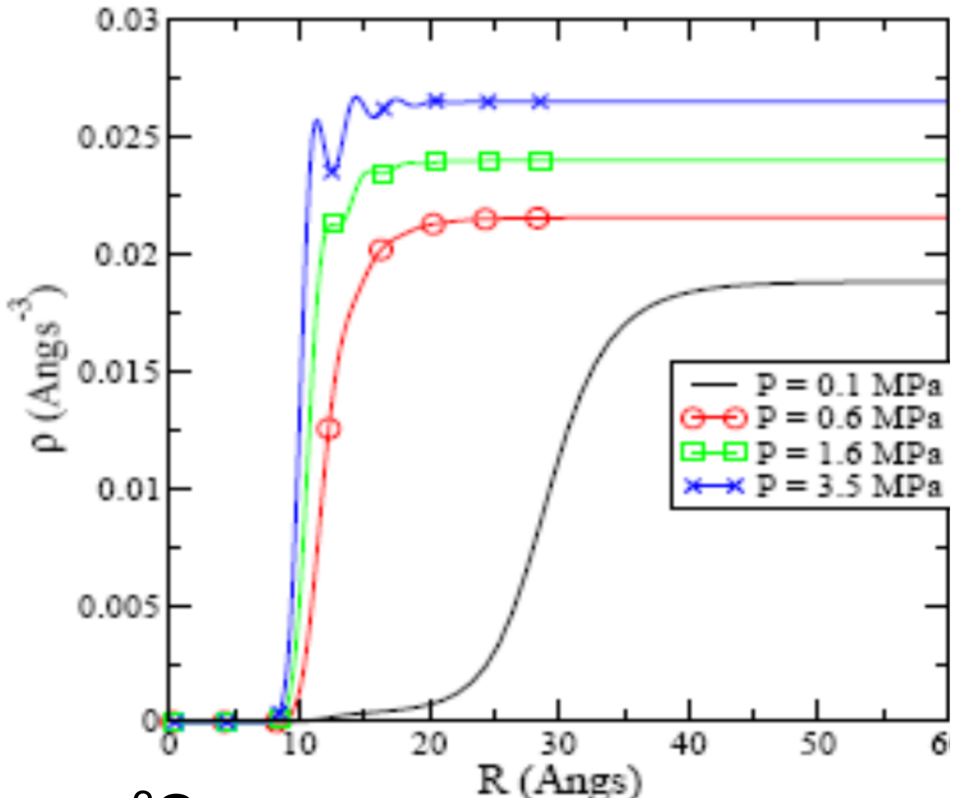

35 bar

Phys. Rev. A 85 042706 (2012).

1 bar

Bubble Radius (R_b) depends on applied pressure (**P**).

^{3}S

Empty cavity around excited atom (emitter)

706.5 nm He* line (^3S-^3P)

Experimental (continuous) vs theoretical (dashed)

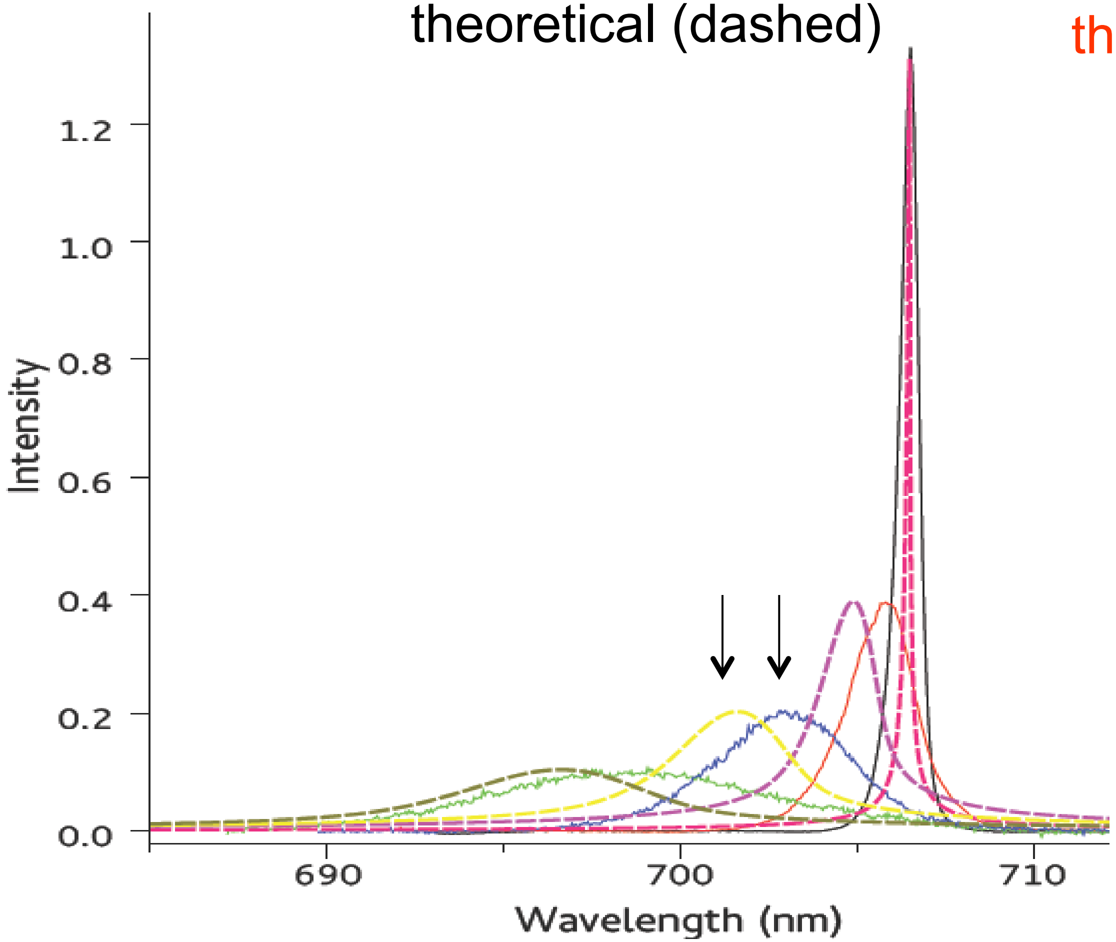

the line position is extremely sensitive to the He*(3s) - He pair potential

Line shift

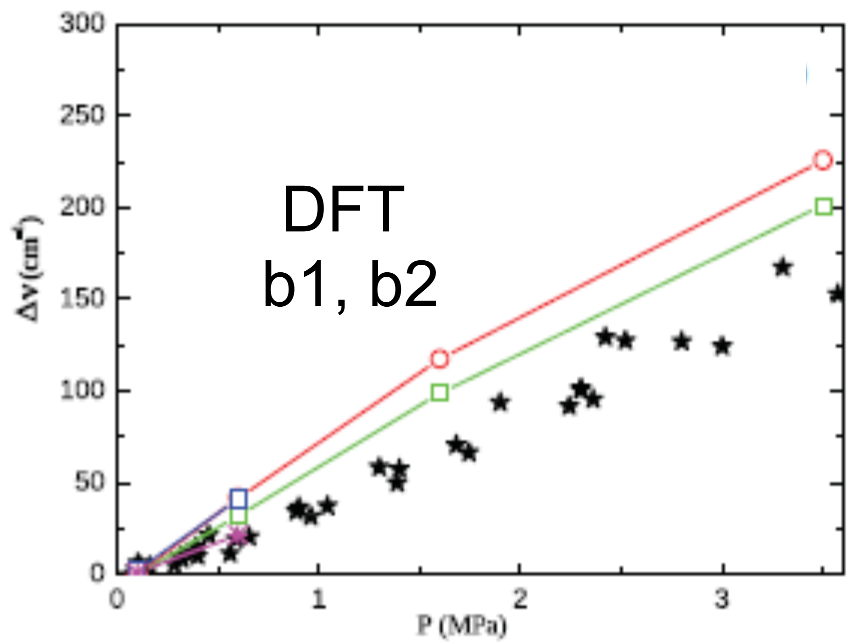

$He_2^*(d^3\Sigma_u)$-He ab initio potential

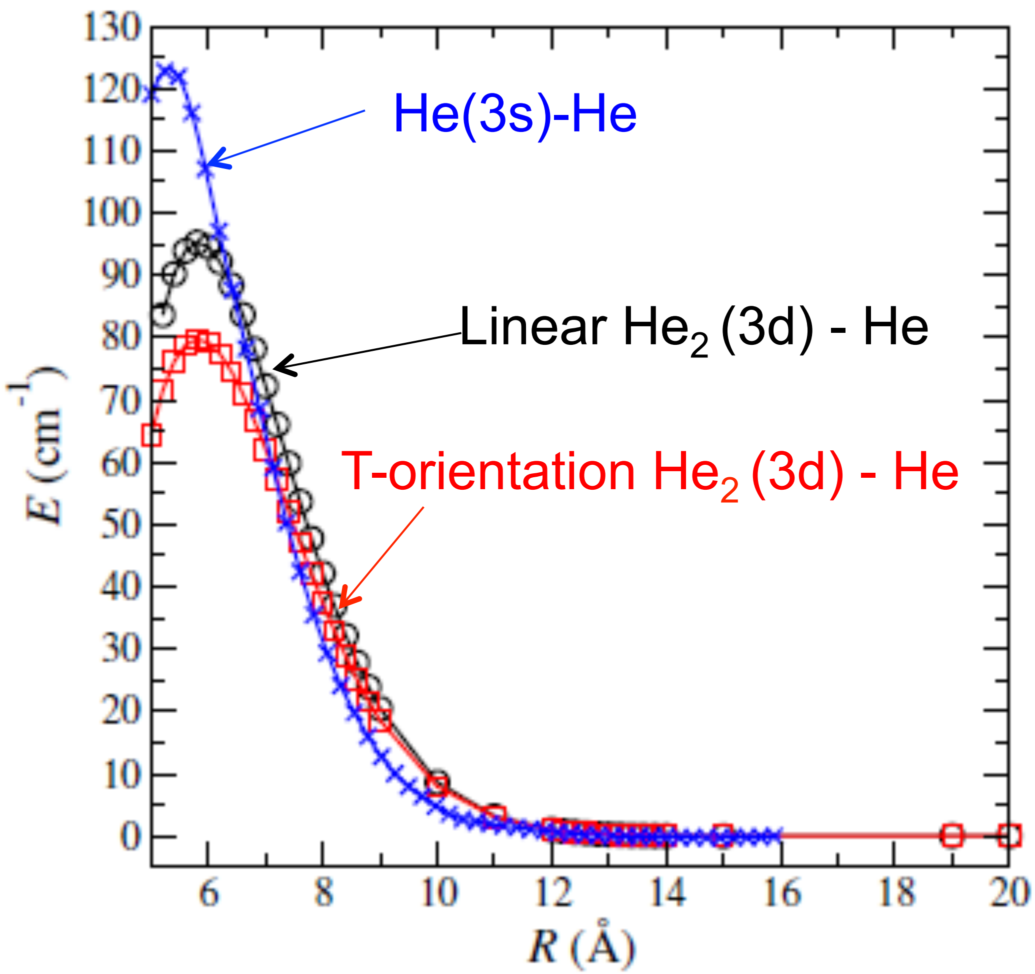

J. Eloranta and V. A. Apkarian
J. Chem. Phys. 115, 752 (2001).

N Bonifaci, Z Li, J Eloranta and S L Fiedler
J. Phys. Chem. A, 120 (45), pp 9019–9027 2016

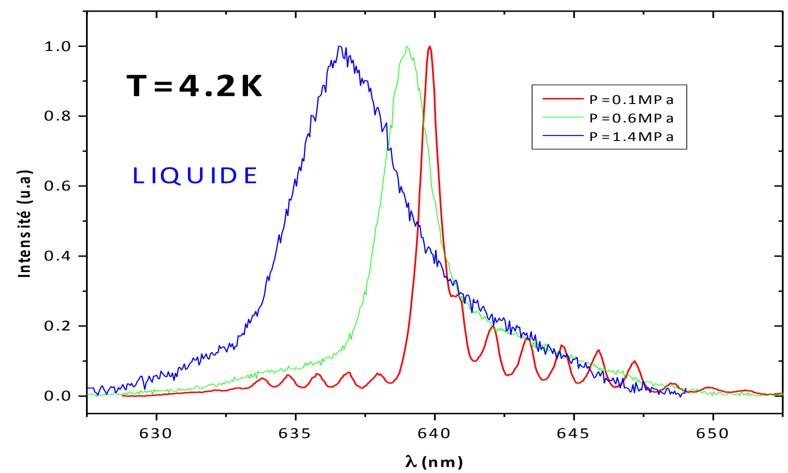

Liquid density around $He_2\ d^3\Sigma_u^+$

DFT

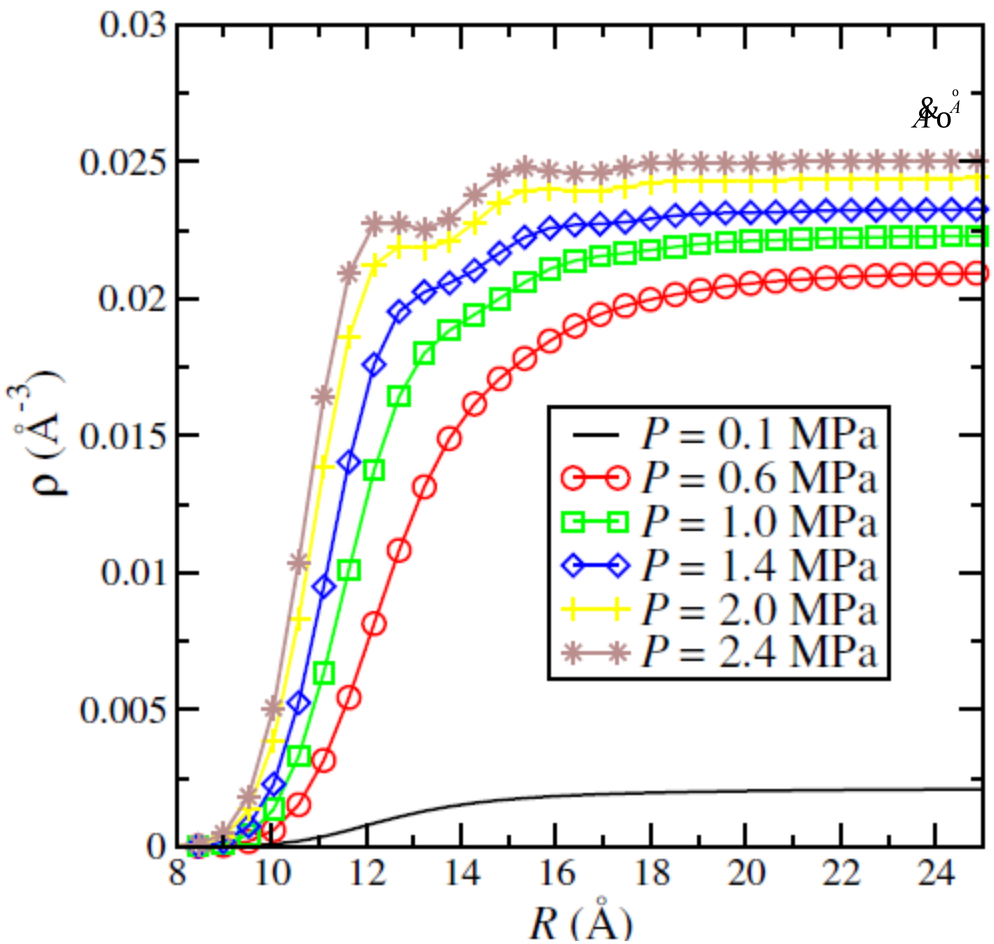

$He_2(^3d\text{-}^3b)$

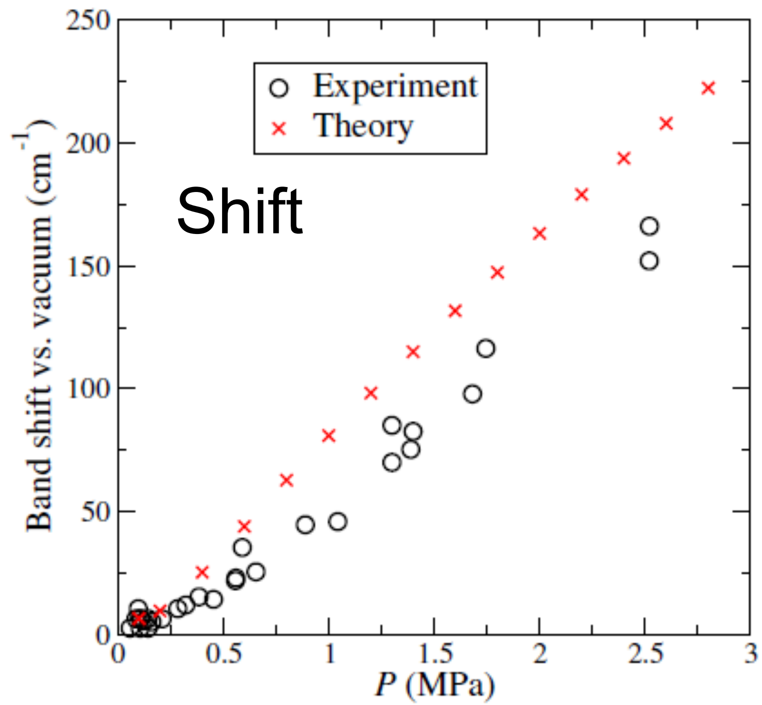

R=12,7 Å 1 Bar
R= 10,8 Å 24 Bar

Conclusion

300 K → 4.2 K

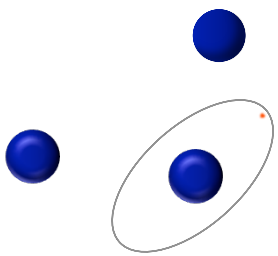

Impact theory

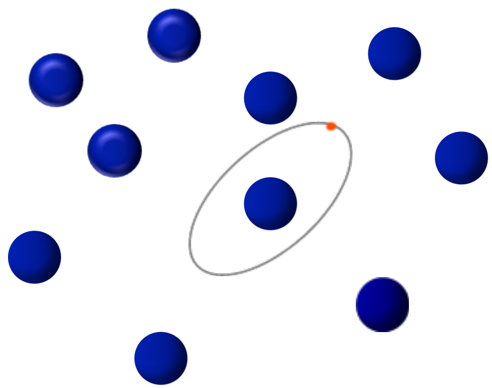

Unified semiclassical theory

N_{He}, N_e, T

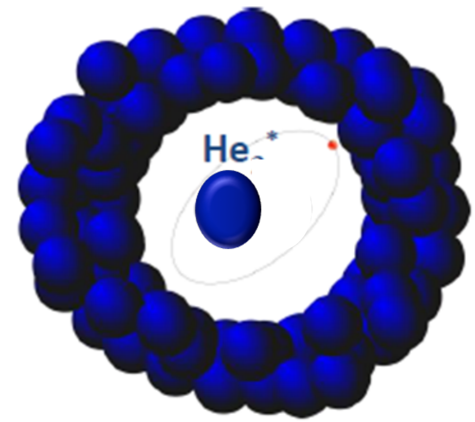

Localized bubble state

	Liquid Helium
He 3s	Bubble R~10 Å
He_2 $d^3\Sigma_u^+$	Bubble R~10-13 Å

The good agreement observed between the simulations and the experimental fluorescence data suggests that both He_2 and He emit from a liquid environment at 4 K.

Outlook: Comparison between Andronikashvili's and the molecular probe

300 K 4 K 1 K

Superfluid phase

Interaction of **He_2^* molecules** with helium → nanoscopic probes $T\lambda$=2,17 K

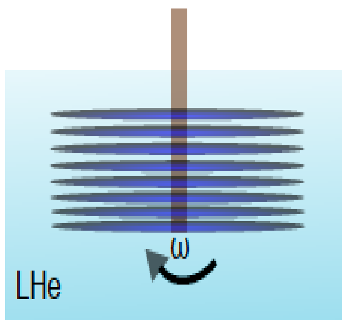

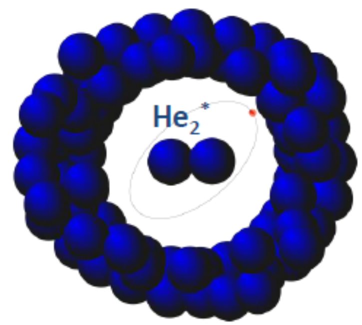

Andronikashvili's experiment	Molecules He_2^*/liquid He
Macroscopic	Microscopic
Two-fluid model	Local two-fluid model
Observable: torsional frequency	Observable : OES

Thank you for your attention